PLANE WAVE DISCONTINUOUS GALERKIN METHODS: ANALYSIS OF THE h-VERSION [*,**]

CLAUDE J. GITTELSON[1], RALF HIPTMAIR[1] AND ILARIA PERUGIA[2]

Abstract. We are concerned with a finite element approximation for time-harmonic wave propagation governed by the Helmholtz equation. The usually oscillatory behavior of solutions, along with numerical dispersion, render standard finite element methods grossly inefficient already in medium-frequency regimes. As an alternative, methods that incorporate information about the solution in the form of plane waves have been proposed. We focus on a class of Trefftz-type discontinuous Galerkin methods that employs trial and test spaces spanned by local plane waves. In this paper we give *a priori* convergence estimates for the h-version of these plane wave discontinuous Galerkin methods in two dimensions. To that end, we develop new inverse and approximation estimates for plane waves and use these in the context of duality techniques. Asymptotic optimality of the method in a mesh dependent norm can be established. However, the estimates require a minimal resolution of the mesh beyond what it takes to resolve the wavelength. We give numerical evidence that this requirement cannot be dispensed with. It reflects the presence of numerical dispersion.

Mathematics Subject Classification. 65N15, 65N30, 35J05.

1. INTRODUCTION

This paper is devoted to the numerical analysis of volumetric discretization schemes for the following model boundary value problem for the Helmholtz equation:

$$
\begin{aligned}
-\Delta u - \omega^2 u &= f && \text{in } \Omega, \\
\nabla u \cdot \boldsymbol{n} + \mathrm{i}\omega\, u &= g && \text{on } \partial\Omega.
\end{aligned}
\tag{1.1}
$$

Here, Ω is a bounded polygonal/polyhedral Lipschitz domain in $\mathbb{R}^d$, $d = 2, 3$, and $\omega > 0$ denotes a fixed wave number (the corresponding wavelength is $\lambda = 2\pi/\omega$). The right hand side f is a source term in $L^2(\Omega)$, $\boldsymbol{n}$ is

[1] SAM, ETH Zurich, 8092 Zürich, Switzerland. `giclaude@student.ethz.ch`; `hiptmair@sam.math.ethz.ch`

[2] Dipartimento di Matematica, Università di Pavia, Italy. `ilaria.perugia@unipv.it`

the outer normal unit vector to $\partial\Omega$, and i is the imaginary unit. Inhomogeneous first order absorbing boundary conditions in the form of impedance boundary conditions are used in (1.1), with boundary data $g \in L^2(\partial\Omega)$.

Denoting by $(\cdot, \cdot)$ the standard complex $L^2(\Omega)$-inner product, namely, $(u, v) = \int_\Omega u\,\overline{v}\,\mathrm{d}V$, the variational formulation of (1.1) reads as follows[1]: find $u \in H^1(\Omega)$ such that, for all $v \in H^1(\Omega)$,

$$(\nabla u, \nabla v) - \omega^2(u, v) + \mathrm{i}\omega \int_{\partial\Omega} u\,\overline{v}\,\mathrm{d}S = (f, v) + \int_{\partial\Omega} g\,\overline{v}\,\mathrm{d}S. \qquad (1.2)$$

Existence and uniqueness of solutions of (1.2) are well established, see, *e.g.*, [26], Section 8.1.

The Galerkin discretization of (1.2) by means of standard piecewise polynomial $H^1(\Omega)$-conforming finite elements is straightforward. Yet, it may deliver sufficient accuracy only at prohibitive costs. For two reasons: firstly, solutions of (1.1) tend to oscillate on the scale of the wavelength $\lambda = 2\pi/\omega$, which entails fine meshes or high polynomial degrees in the case of piecewise polynomial approximation. Secondly, low order finite element schemes are also haunted by the so-called *pollution effect*, that is, a widening gap between best approximation error and Galerkin discretization error for increasing wavenumbers, see [4,24]. For spectral Galerkin methods, the dispersion error is controlled at the expense of non-locality of the discretization, see [1]. The pollution effect is closely linked to the notion of *numerical dispersion*: we observe that plane waves $\boldsymbol{x} \mapsto \exp(\mathrm{i}\omega\boldsymbol{d} \cdot \boldsymbol{x})$, $|\boldsymbol{d}| = 1$, are solutions of the homogeneous Helmholtz equation $-\Delta u - \omega^2 u = 0$; when the discretized operator is examined (in a periodic setting), its kernel functions turn out to be similar plane waves but with a different wavelength.

It is a natural idea to incorporate "knowledge" about both the oscillatory character of solutions and their intrinsic wavelength into a discretization of (1.1). This has been pursued in many ways, mainly by building trial spaces based on plane waves. This has been attempted in the partition of unity (PUM) finite element method [3,20,25,26,28], the discontinuous enrichment approach [14,15,33], in the context of least squares approaches [27,32], and in the so-called "Variational Theory of Complex Rays" (VTCR) approach [29].

Arguably, the most "exotic" among the plane wave methods is the ultra-weak variational formulation (UWVF) introduced by Cessenat and Després [9–11,13]. It owes its name to the twofold integration by parts underlying its original formulation, which features impedance traces on cell boundaries as unknowns in the variational formulation. Cessenat and Després managed to establish existence and uniqueness of solutions of the UWVF, but failed to give meaningful *a priori* error estimates. On the other hand, extensive numerical experiments mainly conducted by Monk and collaborators indicate reliable convergence [21,22] for a wide range of wave propagation problems (without volume sources). This carries over to the extension of the method to Maxwell's equations [9,23].

Fresh analysis was made possible by the discovery that the UWVF can be recast as a special discontinuous Galerkin (DG) method for (1.1) with trial and test spaces supplied by local plane wave spaces. This relationship gradually emerged, *cf.* [17,23], and is made fully explicit in Section 2 of this article and in a paper by Buffa and Monk [7], which was written parallel to ours, see Remark 4.15 for a discussion of its results. The big gain from this new perspective is that powerful techniques of DG analysis can be harnessed for understanding the convergence properties of the UWVF. This was done in [7] building on estimates already established by Cessenat and Després. In the present paper the relationship of UWVF and DG paves the way for adapting the convergence theory of elliptic DG methods [8] combined with duality techniques [5,30]. We point out that this entailed a slight modification of the UWVF in order to enhance its stability.

Thus, we obtain *a priori* h-asymptotic estimates in both a mesh-dependent broken H^1-norm and the L^2-norm, see Section 4. The estimates target the case of uniform mesh refinement keeping the resolution of local trial spaces fixed, the so-called h-version of volumetric discretization schemes. h-asymptotic quasi-optimality with ω-uniform constants is established, which predicts algebraic convergence of the plane wave DG solutions as the global meshwidth h tends to 0. However, the estimates hinge on the daunting assumption that

---

[1]For a bounded domain $D \subset \mathbb{R}^d$, $d = 1, 2, 3$, we denote by $H^s(D)$, $s \in \mathbb{N}_0$, the standard Sobolev space of order s of complex-valued functions, and by $\|\cdot\|_{s,D}$ the usual Sobolev norm. For $s = 0$, we write $L^2(D)$ in lieu of $H^0(D)$. We also use $\|\cdot\|_{s,D}$ to denote the norm for the space $(H^s(D))^d$.

$h\omega^2\text{diam}(\Omega)$ is sufficiently small, which amounts to the pollution effect rearing its head again. Basically we end up with the same requirement of over-resolving the wavelength as stipulated by the usual error estimates for piecewise linear globally continuous finite elements.

In short, our theory does not support the claim that the h-version of plane wave DG methods is immune to the pollution effect. Simple numerical experiments send the same message, see Section 5. Nevertheless plane wave DG method for (1.1) can be viable when used wisely. It is not advisable to try and improve accuracy by refining the mesh. Rather, the cell size should be linked to the wavelength and the number of plane wave directions should be increased. In fact, it is large cells and large local spaces that are preferred in practical applications of the method.

Hence, the asymptotics considered in the present paper and in [7,10] may not be the relevant. Nevertheless, we believe that investigation of h-version convergence is an essential first step in understanding the more interesting p-version of plane wave Galerkin methods. Moreover, already the case of h-refinement forced us to develop some theoretical tools which are certainly of interest in their own right: (i) construction of a basis for plane wave spaces that remains stable for small wavenumbers (see Sect. 3.1); (ii) inverse estimates and projection error estimates for plane waves (see Sect. 3.2); (iii) new variants of duality arguments (see Sect. 4).

The outline of the paper is as follows: in Section 2 we derive a (primal) mixed DG variational formulation of (1.1) with Trefftz type local trial spaces. We specify numerical fluxes and make the connection to UWVF. Section 3 contains the definition of a stable basis for plane wave spaces and some related key results (inverse and projection error estimates) used in the convergence analysis developed in Section 4. Key duality estimates rely on elliptic lifting theorems for Helmholtz boundary value problems (see [12,19,26]). For the moment our analysis is confined to $d = 2$. We believe that it can be extended to $d = 3$ without substantial modifications. Finally, numerical results that demonstrate that our estimates for h-convergence rates are sharp are presented in Section 5.

2. Discontinuous Galerkin approach

To begin with, we follow the general approach to the derivation of discontinuous Galerkin schemes for second-order elliptic boundary value problems presented in [8]: Let $\mathcal{T}_h$ be a partition of Ω into polyhedral subdomains K of diameters h_K with possible hanging nodes. Let $\mathcal{F}_h$ be the skeleton of the partition $\mathcal{T}_h$, and define $\mathcal{F}_h^{\mathcal{B}} = \mathcal{F}_h \cap \partial\Omega$ and $\mathcal{F}_h^{\mathcal{I}} = \mathcal{F}_h \setminus \mathcal{F}_h^{\mathcal{B}}$. We introduce the auxiliary variable $\boldsymbol{\sigma} := \nabla u/\mathrm{i}\omega$ and write problem (1.1) as a first order system:

$$\begin{aligned}
\mathrm{i}\omega\,\boldsymbol{\sigma} &= \nabla u && \text{in } \Omega, \\
\mathrm{i}\omega\,u - \nabla\cdot\boldsymbol{\sigma} &= \frac{1}{\mathrm{i}\omega}\,f && \text{in } \Omega, \\
\mathrm{i}\omega\boldsymbol{\sigma}\cdot\boldsymbol{n} + \mathrm{i}\omega\,u &= g && \text{on } \partial\Omega.
\end{aligned} \tag{2.1}$$

Now, introduce a partition $\mathcal{T}_h$ of Ω into subdomains K, and proceed as in [8]. By multiplying the first and second equation of (2.1) by smooth test functions $\boldsymbol{\tau}$ and v, respectively, and integrating by parts on each K, we obtain

$$\int_K \mathrm{i}\omega\,\boldsymbol{\sigma}\cdot\overline{\boldsymbol{\tau}}\,\mathrm{d}V + \int_K u\,\overline{\nabla\cdot\boldsymbol{\tau}}\,\mathrm{d}V - \int_{\partial K} u\,\overline{\boldsymbol{\tau}\cdot\boldsymbol{n}}\,\mathrm{d}S = 0 \quad \forall\boldsymbol{\tau}\in\mathbf{H}(\text{div};K)$$

$$\int_K \mathrm{i}\omega\,u\,\overline{v}\,\mathrm{d}V + \int_K \boldsymbol{\sigma}\cdot\overline{\nabla v}\,\mathrm{d}V - \int_{\partial K} \boldsymbol{\sigma}\cdot\boldsymbol{n}\,\overline{v}\,\mathrm{d}S = \frac{1}{\mathrm{i}\omega}\int_K f\,\overline{v}\,\mathrm{d}V \quad \forall v\in H^1(K). \tag{2.2}$$

Introduce discontinuous *discrete* function spaces $\boldsymbol{\Sigma}_h$ and V_h; replace $\boldsymbol{\sigma},\boldsymbol{\tau}$ by $\boldsymbol{\sigma}_h,\boldsymbol{\tau}_h\in\boldsymbol{\Sigma}_h$ and u,v by $u_h,v_h\in V_h$. Then, approximate the traces of u and $\boldsymbol{\sigma}$ across interelement boundaries by the so-called *numerical fluxes*

denoted by $\widehat{u}_h$ and $\widehat{\boldsymbol{\sigma}}_h$, respectively (see, *e.g.*, [2] for details) and obtain

$$\int_K \mathrm{i}\omega\,\boldsymbol{\sigma}_h \cdot \overline{\boldsymbol{\tau}}_h\,\mathrm{d}V + \int_K u_h\,\overline{\nabla \cdot \boldsymbol{\tau}}_h\,\mathrm{d}V - \int_{\partial K} \widehat{u}_h\,\overline{\boldsymbol{\tau}_h \cdot \boldsymbol{n}}\,\mathrm{d}S = 0 \quad \forall \boldsymbol{\tau}_h \in \boldsymbol{\Sigma}_h(K)$$

$$\int_K \mathrm{i}\omega\,u_h\,\overline{v}_h\,\mathrm{d}V + \int_K \boldsymbol{\sigma}_h \cdot \overline{\nabla v}_h\,\mathrm{d}V - \int_{\partial K} \widehat{\boldsymbol{\sigma}}_h \cdot \boldsymbol{n}\,\overline{v}_h\,\mathrm{d}S = \frac{1}{\mathrm{i}\omega}\int_K f\,\overline{v}_h\,\mathrm{d}V \quad \forall v_h \in V_h(K). \tag{2.3}$$

At this point, in order to complete the the definition of classical DG methods, one "simply" needs to choose the numerical fluxes $\widehat{u}_h$ and $\widehat{\boldsymbol{\sigma}}_h$ (notice that only the normal component of $\widehat{\boldsymbol{\sigma}}_h$ is needed).

In light of our special choice of V_h and $\boldsymbol{\Sigma}_h$ explained below, we reverse integration by parts in the first equation of (2.3):

$$\int_K \boldsymbol{\sigma}_h \cdot \overline{\boldsymbol{\tau}}_h\,\mathrm{d}V = \frac{1}{\mathrm{i}\omega}\int_K \nabla u_h \cdot \overline{\boldsymbol{\tau}}_h\,\mathrm{d}V - \frac{1}{\mathrm{i}\omega}\int_{\partial K}(u_h - \widehat{u}_h)\,\overline{\boldsymbol{\tau}_h \cdot \boldsymbol{n}}\,\mathrm{d}S. \tag{2.4}$$

Assume $\nabla_h V_h \subseteq \boldsymbol{\Sigma}_h$ and take $\boldsymbol{\tau}_h = \nabla v_h$ in each element. Insert the resulting expression for $\int_K \boldsymbol{\sigma}_h \cdot \overline{\nabla v}_h\,\mathrm{d}V$ into the second equation of (2.3). We get

$$\int_K (\nabla u_h \cdot \nabla \overline{v}_h - \omega^2 u_h \overline{v}_h)\,\mathrm{d}V - \int_{\partial K}(u_h - \widehat{u}_h)\,\overline{\nabla v_h \cdot \boldsymbol{n}}\,\mathrm{d}S - \int_{\partial K} \mathrm{i}\omega\widehat{\boldsymbol{\sigma}}_h \cdot \boldsymbol{n}\,\overline{v}_h\,\mathrm{d}S = \int_K f\,\overline{v}_h\,\mathrm{d}V. \tag{2.5}$$

Notice that the formulation (2.5) is equivalent to (2.3) in the sense that their u_h solution components coincide and the $\boldsymbol{\sigma}_h$ solution component of (2.3) can be recovered from u_h by using (2.4).

Another equivalent formulation can be obtained by integrating by parts once more the first term in (2.5) (notice that the boundary term appearing in this integration by parts cancels out with a boundary term already present in (2.5)):

$$\int_K (\overline{-\Delta v_h - \omega^2 v_h})\,u_h\,\mathrm{d}V + \int_{\partial K} \widehat{u}_h\,\overline{\nabla v_h \cdot \boldsymbol{n}}\,\mathrm{d}S - \int_{\partial K} \mathrm{i}\omega\widehat{\boldsymbol{\sigma}}_h \cdot \boldsymbol{n}\,\overline{v}_h\,\mathrm{d}S = \int_K f\,\overline{v}_h\,\mathrm{d}V. \tag{2.6}$$

By taking *Trefftz-type test functions* v_h in (2.6) such that, for all $K \in \mathcal{T}_h$,

$$-\Delta v_h - \omega^2 v_h = 0 \qquad \text{in } K,$$

equation (2.6) simply becomes

$$\int_{\partial K} \widehat{u}_h\,\overline{\nabla v_h \cdot \boldsymbol{n}}\,\mathrm{d}S - \int_{\partial K} \mathrm{i}\omega\widehat{\boldsymbol{\sigma}}_h \cdot \boldsymbol{n}\,\overline{v}_h\,\mathrm{d}S = \int_K f\,\overline{v}_h\,\mathrm{d}V. \tag{2.7}$$

To discuss concrete choices for the numerical fluxes, it is convenient to adopt the notations used in the description of discontinuous Galerkin methods: let u_h and $\boldsymbol{\sigma}_h$ be a piecewise smooth function and vector field on $\mathcal{T}_h$, respectively. On $\partial K^- \cap \partial K^+$, we define

$$\text{the averages:} \quad \{\!\{u_h\}\!\} := \tfrac{1}{2}(u_h^+ + u_h^-), \quad \{\!\{\boldsymbol{\sigma}_h\}\!\} := \tfrac{1}{2}(\boldsymbol{\sigma}_h^+ + \boldsymbol{\sigma}_h^-),$$
$$\text{the jumps:} \quad [\![u_h]\!]_N := u_h^+ \boldsymbol{n}^+ + u_h^- \boldsymbol{n}^-, \quad [\![\boldsymbol{\sigma}_h]\!]_N := \boldsymbol{\sigma}_h^+ \cdot \boldsymbol{n}^+ + \boldsymbol{\sigma}_h^- \cdot \boldsymbol{n}^-.$$

Now, we build numerical fluxes by multiplying $[\![u_h]\!]_N$ and $[\![\nabla_h u_h]\!]_N$ in (2.10) with mesh dependent coefficients. In order to do that, we define the local mesh size function $\mathtt{h}$ on $\mathcal{F}_h^{\mathcal{I}}$ by $\mathtt{h}(\boldsymbol{x}) = \min\{h_{K^-}, h_{K^+}\}$ if $\boldsymbol{x}$ is in the interior

of $\partial K^- \cap \partial K^+$. Mimicking the general form of numerical fluxes introduced in [8], the primal formulation we will analyze is obtained by choosing the numerical fluxes in (2.7) as follows: on $\partial K^- \cap \partial K^+ \subset \mathcal{F}_h^{\mathcal{I}}$, we define

$$\widehat{\boldsymbol{\sigma}}_h = \frac{1}{\mathrm{i}\omega}\{\!\!\{\nabla_h u_h\}\!\!\} - \alpha \, [\![u_h]\!]_N - \frac{\gamma}{\mathrm{i}\omega} \, [\![\nabla_h u_h]\!]_N,$$

$$\widehat{u}_h = \{\!\!\{u_h\}\!\!\} + \boldsymbol{\gamma} \cdot [\![u_h]\!]_N - \frac{\beta}{\mathrm{i}\omega} \, [\![\nabla_h u_h]\!]_N, \tag{2.8}$$

and on $\partial K \cap \partial\Omega \subset \mathcal{F}_h^{\mathcal{B}}$, we define

$$\widehat{\boldsymbol{\sigma}}_h = \frac{1}{\mathrm{i}\omega}\nabla_h u_h - (1-\delta)\left(\frac{1}{\mathrm{i}\omega}\nabla_h u_h + u_h\,\boldsymbol{n} - \frac{1}{\mathrm{i}\omega}g\,\boldsymbol{n}\right),$$

$$\widehat{u}_h = u_h - \delta\left(\frac{1}{\mathrm{i}\omega}\nabla_h u_h \cdot \boldsymbol{n} + u_h - \frac{1}{\mathrm{i}\omega}g\right), \tag{2.9}$$

with parameters $\alpha > 0$, $\beta \geq 0$, $\boldsymbol{\gamma}$ and $0 < \delta < 1$ to be chosen. Here and in the following, the symbol ∇_h stands for the elementwise application of the operator ∇.

Remark 2.1. The ultra-weak variational formulation (UWVF) of Cessenat and Després, see [10,11], is obtained by choosing the numerical fluxes in (2.7) as follows: on $\partial K^- \cap \partial K^+ \subset \mathcal{F}_h^{\mathcal{I}}$, we define

$$\widehat{\boldsymbol{\sigma}}_h = \frac{1}{\mathrm{i}\omega}\{\!\!\{\nabla_h u_h\}\!\!\} - \frac{1}{2}\,[\![u_h]\!]_N,$$

$$\widehat{u}_h = \{\!\!\{u_h\}\!\!\} - \frac{1}{2\mathrm{i}\omega}\,[\![\nabla_h u_h]\!]_N, \tag{2.10}$$

and on $\partial K \cap \partial\Omega \subset \mathcal{F}_h^{\mathcal{B}}$, we define

$$\widehat{\boldsymbol{\sigma}}_h = \frac{1}{\mathrm{i}\omega}\nabla_h u_h - \frac{1}{2}\left(\frac{1}{\mathrm{i}\omega}\nabla_h u_h + u_h\,\boldsymbol{n} - \frac{1}{\mathrm{i}\omega}g\,\boldsymbol{n}\right),$$

$$\widehat{u}_h = u_h - \frac{1}{2}\left(\frac{1}{\mathrm{i}\omega}\nabla_h u_h \cdot \boldsymbol{n} + u_h - \frac{1}{\mathrm{i}\omega}g\right). \tag{2.11}$$

In fact, multiply equation (2.7) by $2\mathrm{i}\omega$ and sum over all elements:

$$\sum_{K\in\mathcal{T}_h}\int_{\partial K}\left(2\mathrm{i}\omega\widehat{u}_h\,\overline{\nabla v_h \cdot \boldsymbol{n}} + 2\mathrm{i}\omega\widehat{\boldsymbol{\sigma}}_h \cdot \boldsymbol{n}\,\overline{\mathrm{i}\omega v_h}\right)\,\mathrm{d}S = 2\mathrm{i}\omega(f, v_h).$$

Now, plug in the fluxes defined in (2.10)–(2.11) and, by denoting with the superscript $^{\text{ext}}$ the quantities taken from the neighbors of the considered element K (obviously, $\boldsymbol{n}^{\text{ext}} = -\boldsymbol{n}$), we can write

$$\sum_K\Bigg[\int_{\partial K\setminus\partial\Omega}\Big[(\mathrm{i}\omega u_h + \mathrm{i}\omega u_h^{\text{ext}} - \nabla u_h \cdot \boldsymbol{n} - \nabla u_h^{\text{ext}} \cdot \boldsymbol{n}^{\text{ext}})\overline{\nabla v_h \cdot \boldsymbol{n}}$$

$$+ (\nabla u_h \cdot \boldsymbol{n} - \nabla u_h^{\text{ext}} \cdot \boldsymbol{n}^{\text{ext}} - \mathrm{i}\omega u_h + \mathrm{i}\omega u_h^{\text{ext}})\overline{\mathrm{i}\omega v_h}\Big]\,\mathrm{d}S$$

$$+ \int_{\partial K\cap\partial\Omega}\Big[(\mathrm{i}\omega u_h - \nabla u_h \cdot \boldsymbol{n} + g)\overline{\nabla v_h \cdot \boldsymbol{n}} + (\nabla u_h \cdot \boldsymbol{n} - \mathrm{i}\omega u_h + g)\overline{\mathrm{i}\omega v_h}\Big]\,\mathrm{d}S\Bigg] = 2\mathrm{i}\omega(f, v_h).$$

From this, by rearranging the terms, we obtain the variational formulation: find $u_h \in V_h$ such that, for all $v_h \in V_h$,

$$\sum_{K \in \mathcal{T}_h} \int_{\partial K} (-\nabla u_h \cdot \boldsymbol{n} + \mathrm{i}\omega u_h)(\overline{-\nabla v_h \cdot \boldsymbol{n} + \mathrm{i}\omega v_h}) \, \mathrm{d}S - \int_{\mathcal{F}_h^{\mathcal{I}}} (-\nabla u_h^- \cdot \boldsymbol{n}^- + \mathrm{i}\omega u_h^-)(\overline{\nabla v_h^+ \cdot \boldsymbol{n}^+ + \mathrm{i}\omega v_h^+}) \, \mathrm{d}S$$

$$- \int_{\mathcal{F}_h^{\mathcal{I}}} (-\nabla u_h^+ \cdot \boldsymbol{n}^+ + \mathrm{i}\omega u_h^+)(\overline{\nabla v_h^- \cdot \boldsymbol{n}^- + \mathrm{i}\omega v_h^-}) \, \mathrm{d}S = -2\mathrm{i}\omega \, (f, v_h) + \int_{\mathcal{F}_h^{\mathcal{B}}} g(\overline{\nabla v_h \cdot \boldsymbol{n} + \mathrm{i}\omega v_h}) \, \mathrm{d}S, \qquad (2.12)$$

where the superscripts $^+$ and $^-$ refer to quantities from the two different elements sharing the considered interior face. This agrees with usual statement of the UWVF in terms of unknown functions on $\mathcal{F}_h$, see [7], Formula 19, [10], Formula (1.4), and [22], Formula 10.

Matching (2.8), (2.9), and (2.10), (2.11), we see that the original UWVF by Cessenat and Després [10] is recovered by choosing

$$\alpha = 1/2, \qquad \beta = 1/2, \qquad \boldsymbol{\gamma} = \boldsymbol{0}, \qquad \delta = 1/2.$$

Following [16,17,23], it is also possible to show that the method by Cessenat and Després can also be recovered by writing the second order problem as a first order system, and then discretizing this system by using a discontinuous Galerkin (DG) method with flux splitting approach (classical upwind DG method). Here, we have followed a slightly different approach and cast the UWVF within the general class of DG methods presented in [8]. A similar perspective was adopted in [7], Section 2.

In order to endow the DG methods with favorable stability properties, the dependence of the coefficients $\alpha, \beta, \boldsymbol{\gamma}$ on the local meshwidth is critical. Our analysis of Section 4 stipulates the following choice of parameters in the definition of the numerical fluxes (2.8) and (2.9)

$$\alpha = \mathtt{a}/\omega\mathtt{h}, \qquad \beta = \mathtt{b}\omega\mathtt{h}, \qquad \boldsymbol{\gamma} = \boldsymbol{0}, \qquad \delta = \mathtt{d}\omega\mathtt{h}, \qquad (2.13)$$

with $\mathtt{a} \geq \mathtt{a}_{\min} > 0$ on $\mathcal{F}_h^{\mathcal{I}}$, $\mathtt{b} \geq 0$ on $\mathcal{F}_h^{\mathcal{I}}$ and $\mathtt{d} > 0$ on $\mathcal{F}_h^{\mathcal{B}}$ (such that $0 < \delta < 1$), all independent of the mesh size and ω. Further assumptions on $\mathtt{a}_{\min}$ and $\mathtt{d}$ will be stated in Section 4. We emphasize that the UWVF does *not* fit (2.13) and, thus, is not covered by the theoretical analysis of this paper.

Remark 2.2. One may also consider the Helmholtz boundary value problem with Dirichlet boundary conditions. In this case, for the boundary condition $u = g_D$ on $\partial\Omega$, the appropriate numerical fluxes for cell faces on $\partial\Omega$ are

$$\widehat{\boldsymbol{\sigma}}_h = \frac{1}{\mathrm{i}\omega} \nabla_h u_h - \lambda \, (u_h \, \boldsymbol{n} - g_D \, \boldsymbol{n}), \quad \widehat{u}_h = g_D, \qquad (2.14)$$

with a parameter $\lambda > 0$. In this case the boundary value problem lacks a unique solution for ω from an infinite discrete set of resonant wave numbers. Thus, we skip pure Dirichlet boundary conditions, as well as pure Neumann boundary conditions, in the convergence analysis.

3. PLANE WAVES

We restrict ourselves to the case $d = 2$ and to triangular meshes. Let $PW_\omega(\mathbb{R}^2)$ be the space of linear combinations of $p \in \mathbb{N}$ plane waves of wavelength $\frac{2\pi}{\omega}$, $\omega > 0$, in $\mathbb{R}^2$, *i.e.*,

$$PW_\omega(\mathbb{R}^2) = \{v \in C^\infty(\mathbb{R}^2) \, : \, v(\boldsymbol{x}) = \sum_{j=1}^p \alpha_j \exp(\mathrm{i}\omega\boldsymbol{d}_j \cdot \boldsymbol{x}), \, \alpha_j \in \mathbb{C}\}, \qquad (3.1)$$

where the directions $\boldsymbol{d}_j \in \mathbb{R}^2$ are fixed, have unit length and are assumed to be different from each other. For simplicity, we suppress the dependence on $\{\boldsymbol{d}_j\}_{j=1}^p$ in the notation for $PW_\omega(\mathbb{R}^2)$. It goes without saying that

every $v \in PW_\omega(\mathbb{R}^2)$ is a solution of the homogeneous Helmholtz equation $-\Delta v - \omega^2 v = 0$ in $\mathbb{R}^2$. From [10], Lemma 2.3, we also learn that, with the abbreviation $e_k := \exp(i\omega d_k \cdot)$ the set $\{e_k\}_{k=1}^p$ is a basis of $PW_\omega(\mathbb{R}^2)$ for all $\omega > 0$.

The drawback of this natural basis is that its vectors become "ever more linearly dependent" as $\omega \to 0$: obviously $e_k \to 1$ if $\omega \to 0$ uniformly on any compact set. For both numerical and theoretical purposes a basis that remains stable for $\omega \to 0$ is needed. The construction of such a basis is carried out in Section 3.1 and inverse and projections estimates for plane wave functions are studied in Section 3.2.

3.1. Stable bases for plane waves

For the direction vectors we may write $d_k := \binom{\cos(\varphi_k)}{\sin(\varphi_k)}$, $\varphi_k \in [0, 2\pi[$, with $\varphi_k \neq \varphi_j$ for $k \neq j$. It is convenient to introduce the symbol

$$\mu_{l,k} := \begin{cases} 1 & \text{for } l = 1, \\ \cos(\frac{l}{2}\varphi_k) & \text{for even } l, \\ \sin(\frac{l-1}{2}\varphi_k) & \text{for odd } l \geq 3, \end{cases} \quad l, k \in \mathbb{N}. \tag{3.2}$$

Let M_p stands for the real $p \times p$-matrix $(\mu_{l,k})_{l,k=1}^p$. For $p = 2m + 1$ it reads

$$M_p := \begin{pmatrix} 1 & 1 & 1 & \cdots & \cdots & 1 \\ \cos(\varphi_1) & \cos(\varphi_2) & \cos(\varphi_3) & \cdots & \cdots & \cos(\varphi_p) \\ \sin(\varphi_1) & \sin(\varphi_2) & \sin(\varphi_3) & \cdots & \cdots & \sin(\varphi_p) \\ \cos(2\varphi_1) & \cos(2\varphi_2) & \cos(2\varphi_3) & \cdots & \cdots & \cos(2\varphi_p) \\ \sin(2\varphi_1) & \sin(2\varphi_2) & \sin(2\varphi_3) & \cdots & \cdots & \sin(2\varphi_p) \\ \vdots & \vdots & \vdots & & & \vdots \\ \cos(m\varphi_1) & \cos(m\varphi_2) & \cos(m\varphi_3) & \cdots & \cdots & \cos(m\varphi_p) \\ \sin(m\varphi_1) & \sin(m\varphi_2) & \sin(m\varphi_3) & \cdots & \cdots & \sin(m\varphi_p) \end{pmatrix}. \tag{3.3}$$

Lemma 3.1. *For odd p the matrix $M_p \in \mathbb{R}^{p,p}$ from (3.3) is regular.*

Proof. If $M_p^T \vec{\zeta} = 0$ for some $\vec{\zeta} \in \mathbb{R}^p$, then

$$\zeta_0 + \sum_{l=1}^m \left[\zeta_{2l-1} \cos(l\varphi_k) + \zeta_{2l} \sin(l\varphi_k) \right] = 0 \quad \text{for } k = 1, \ldots, p.$$

Hence, $\vec{\zeta}$ is the coefficient vector for a real valued trigonometric polynomial of degree m with $2m + 1$ different zeros φ_k, $k = 1, \ldots, p$. This polynomial must be zero everywhere. $\qquad \square$

The inverse of the matrix M_p will effect a transformation to a basis that remains *stable in the limit $\omega \to 0$*. We set $\alpha_k^{(j)} := (M_p^{-1})_{k,j}$, $1 \leq k, j \leq p$, and define

$$b_j := (i\omega)^{-\left[\frac{j}{2}\right]} \sum_{k=1}^p \alpha_k^{(j)} e_k. \tag{3.4}$$

Since M_p is regular, $\{b_j\}_{j=1}^p$ will be a basis of $PW_\omega(\mathbb{R}^2)$, too.

The actual computation of b_j starts from the series expansion of the exponentials

$$\sum_{k=1}^p \alpha_k^{(j)} e_k(x) = \sum_{n=0}^\infty \frac{1}{n!} (i\omega)^n \sum_{k=1}^p \alpha_k^{(j)} (d_k \cdot x)^n, \tag{3.5}$$

where summations may be interchanged due to the uniform convergence of the series. Next, we write $\boldsymbol{x} = \binom{x}{y}$ and use that

$$\left(\begin{pmatrix} \cos\varphi \\ \sin\varphi \end{pmatrix} \cdot \boldsymbol{x}\right)^n = \sum_{j=0}^{n} \binom{n}{j} \cos^{n-j}(\varphi)\sin^j(\varphi)\, x^{n-j}y^j \tag{3.6}$$

is a real trigonometric polynomial of degree n. Thus it can be expressed as a Fourier sum

$$\left(\begin{pmatrix} \cos\varphi \\ \sin\varphi \end{pmatrix} \cdot \boldsymbol{x}\right)^n = \frac{\gamma_0^n(\boldsymbol{x})}{2} + \sum_{j=1}^{n} \left[\gamma_j^n(\boldsymbol{x})\cos(j\varphi) + \sigma_j^n(\boldsymbol{x})\sin(j\varphi)\right], \tag{3.7}$$

where

$$\gamma_j^n(\boldsymbol{x}) = \frac{1}{\pi}\int_{-\pi}^{\pi} \left(\begin{pmatrix} \cos\varphi \\ \sin\varphi \end{pmatrix} \cdot \boldsymbol{x}\right)^n \cos(j\varphi)\, \mathrm{d}\varphi, \quad j = 0,\ldots,n, \tag{3.8}$$

$$\sigma_j^n(\boldsymbol{x}) = \frac{1}{\pi}\int_{-\pi}^{\pi} \left(\begin{pmatrix} \cos\varphi \\ \sin\varphi \end{pmatrix} \cdot \boldsymbol{x}\right)^n \sin(j\varphi)\, \mathrm{d}\varphi, \quad j = 1,\ldots,n. \tag{3.9}$$

From (3.7) is it immediate that both $\gamma_j^n(\boldsymbol{x})$ and $\sigma_j^n(\boldsymbol{x})$ are homogeneous polynomials in x, y. We also find that

$$j + n \text{ odd} \quad \Rightarrow \quad \gamma_j^n(\boldsymbol{x}) = 0, \quad \sigma_j^n(\boldsymbol{x}) = 0. \tag{3.10}$$

In fact, by setting $z = x + \mathrm{i}y$, we can write

$$\left(\begin{pmatrix} \cos\varphi \\ \sin\varphi \end{pmatrix} \cdot \boldsymbol{x}\right)^n = 2^{-n}\sum_{k=0}^{n} \binom{n}{k}\overline{z}^{n-k}z^k \exp(\mathrm{i}(n-2k)\varphi).$$

Therefore, for even n, $\left(\begin{pmatrix} \cos\varphi \\ \sin\varphi \end{pmatrix} \cdot \boldsymbol{x}\right)^n$ has vanishing Fourier coefficients for odd indices, whereas, for odd n, it has vanishing Fourier coefficients for even indices. Formula (3.10) follows from the the fact that σ_j^n and γ_j^n are such trigonometric Fourier coefficients; see (3.7).

Moreover, for any $n \in \mathbb{N}$, the nonzero $\gamma_j^n(\boldsymbol{x})$, $\sigma_j^n(\boldsymbol{x})$ provide a basis of the space of two-variate homogeneous polynomials of degree n.

For the sake of simplicity, we set $\kappa_1^n(\boldsymbol{x}) := \gamma_0^n(\boldsymbol{x})/2$, $\kappa_{2j}^n(\boldsymbol{x}) := \gamma_j^n(\boldsymbol{x})$, $j = 1,\ldots,n$, for even j, and $\kappa_{2j+1}^n(\boldsymbol{x}) := \sigma_j^n(\boldsymbol{x})$ for odd j. Using (3.2) this permits us to rewrite

$$\left(\begin{pmatrix} \cos\varphi_k \\ \sin\varphi_k \end{pmatrix} \cdot \boldsymbol{x}\right)^n = \sum_{l=1}^{2n+1} \kappa_l^n(\boldsymbol{x})\mu_{l,k}. \tag{3.11}$$

We plug this into (3.5), change order of summation,

$$\sum_{k=1}^{p} \alpha_k^{(j)} e_k(\boldsymbol{x}) = \sum_{n=0}^{\infty}\left(\frac{1}{n!}(\mathrm{i}\omega)^n \sum_{k=1}^{p}\left(\alpha_k^{(j)}\sum_{l=1}^{2n+1}\kappa_l^n(\boldsymbol{x})\mu_{l,k}\right)\right) = \sum_{n=0}^{\infty}\left(\frac{1}{n!}(\mathrm{i}\omega)^n \sum_{l=1}^{2n+1}\left(\kappa_l^n(\boldsymbol{x})\sum_{k=1}^{p}\alpha_k^{(j)}\mu_{l,k}\right)\right),$$

and observe that, by definition of $\alpha_k^{(j)}$,

$$\sum_{k=1}^{p} \alpha_k^{(j)}\mu_{l,k} = \delta_{lj} := \begin{cases} 1 & \text{if } l = j, \\ 0 & \text{else}, \end{cases} \qquad \text{for} \quad 1 \le l, j \le p.$$

Using this formula for $n = 0, \ldots, m$, and splitting the outer sum accordingly, we infer

$$\sum_{k=1}^{p} \alpha_k^{(j)} e_k(\boldsymbol{x}) = \sum_{n=\left[\frac{j}{2}\right]}^{m} \frac{1}{n!} (\mathrm{i}\omega)^n \kappa_j^n(\boldsymbol{x}) + \sum_{n=m+1}^{\infty} \left\{ \frac{1}{n!} (\mathrm{i}\omega)^n \left(\kappa_j^n(\boldsymbol{x}) + \sum_{l=p+1}^{2n+1} \kappa_l^n(\boldsymbol{x}) \sum_{k=1}^{p} \alpha_k^{(j)} \mu_{l,k} \right) \right\}.$$

This means

$$b_j(\boldsymbol{x}) = \sum_{n=\left[\frac{j}{2}\right]}^{m} \frac{1}{n!} (\mathrm{i}\omega)^{n-\left[\frac{j}{2}\right]} \kappa_j^n(\boldsymbol{x}) + \omega^{m+1-\left[\frac{j}{2}\right]} R_j(\omega, \boldsymbol{x}), \tag{3.12}$$

with a remainder function $R_j(\omega, \boldsymbol{x})$ that, thanks to $|\kappa_j^n(\boldsymbol{x})| \leq 2|\boldsymbol{x}|^n$, is uniformly bounded on compact sets. This immediately gives

$$\lim_{\omega \to 0} b_j(\boldsymbol{x}) = \frac{1}{\left[\frac{j}{2}\right]!} \kappa_j^{\left[\frac{j}{2}\right]}(\boldsymbol{x}). \tag{3.13}$$

Unraveling the definition of κ_j^n, we find

$$\kappa_1^0 = \tfrac{1}{2}\gamma_0^0 \equiv 1, \quad \kappa_j^{\left[\frac{j}{2}\right]} = \gamma_{\frac{j}{2}}^{\frac{j}{2}} \quad \text{for even } j, \quad \kappa_j^{\left[\frac{j}{2}\right]} = \sigma_{\frac{j-1}{2}}^{\frac{j-1}{2}} \quad \text{for odd } j \geq 3.$$

This links the limits to the integrals

$$\frac{1}{\pi} \int_{-\pi}^{\pi} (x \cos \varphi + y \sin \varphi)^n \exp(\mathrm{i}n\varphi) \, \mathrm{d}\varphi = \frac{1}{\pi} \int_{-\pi}^{\pi} \frac{1}{2^n} (\exp(\mathrm{i}\varphi)\overline{z} + \exp(-\mathrm{i}\varphi)z)^n \exp(\mathrm{i}n\varphi) \, \mathrm{d}\varphi$$

$$= \frac{1}{2^n \pi} \int_{-\pi}^{\pi} \sum_{l=0}^{n} \binom{n}{l} \overline{z}^l z^{n-l} \exp(\mathrm{i}2l\varphi) \, \mathrm{d}\varphi$$

$$= \frac{1}{2^{n-1}} z^n, \quad \text{with} \quad z = x + \mathrm{i}y, \quad n \in \mathbb{N},$$

which gives us

$$\kappa_j^{\left[\frac{j}{2}\right]}(\boldsymbol{x}) = 2^{1-\left[\frac{j}{2}\right]} \left\{ \begin{matrix} \mathrm{Re} \\ \mathrm{Im} \end{matrix} \right\} (x + \mathrm{i}y)^{\left[\frac{j}{2}\right]}, \quad \left\{ \begin{matrix} \text{for even } j, \\ \text{for odd } j. \end{matrix} \right. \tag{3.14}$$

So the basis functions b_j tend to scaled standard harmonic polynomials in the limit $\omega \to 0$:

$$\left\{ b_j^0(\boldsymbol{x}) := \lim_{\omega \to 0} b_j(\boldsymbol{x}) \right\}_{j=1}^{p} = \left\{ 1, \frac{2^{1-k}}{k!} \mathrm{Re}(x + \mathrm{i}y)^k, \frac{2^{1-k}}{k!} \mathrm{Im}(x + \mathrm{i}y)^k \right\}_{k=1}^{m}. \tag{3.15}$$

Those are, of course, linearly independent. Thus, we retain linear independence of the functions in the limit $\omega \to 0$.

Remark 3.2. The number p of plane waves being odd is essential. In fact, with even p, one would end up with an incomplete space of harmonic polynomials in the limit $\omega \to 0$; see (3.15). Moreover, for even p, the matrix $\boldsymbol{M}_p$ from (3.3) can be singular (take, e.g., $p = 2$, $0 < \varphi_1 < 2\pi$ and $\varphi_2 = 2\pi - \varphi_1$) and the definition of the stable basis functions is no longer valid.
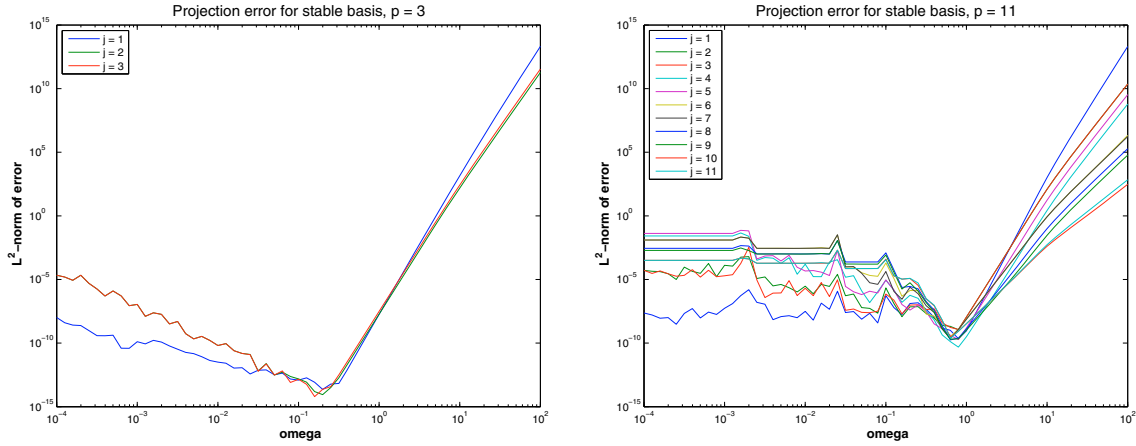
FIGURE 1. Residual norm for L^2 projection of truncated basis functions b_j onto plane wave space on the unit square $[0,1]^2$. Truncation after 13 terms in the expansion w.r.t. ω.

Now, we take for granted that the directions $\boldsymbol{d}_j$ are uniformly spaced on the circle, that is,

$$\boldsymbol{d}_j = \begin{pmatrix} \cos(\frac{2\pi}{p}(j-1)+\xi) \\ \sin(\frac{2\pi}{p}(j-1)+\xi) \end{pmatrix}, \quad j = 1,\ldots,p, \quad \xi \in \mathbb{R}. \tag{3.16}$$

This is the customary choice, which is also made in the standard ultra weak discontinuous Galerkin formulation. The special plane wave space distinguished by equispaced directions (3.16) will be designated by $PW_\omega^{p,\xi}(\mathbb{R}^2)$.

Lemma 3.3. *For the particular choice* $\varphi_j = \frac{2\pi}{p}(j-1)+\xi$, $j = 1,\ldots,p$, $\xi \in \mathbb{R}$*, the matrix* $\boldsymbol{M}_p$ *from* (3.3) *satisfies* $\boldsymbol{M}_p \boldsymbol{M}_p^T = \mathrm{diag}(p, \frac{1}{2}p, \ldots, \frac{1}{2}p)$.

Proof. The assertion of the lemma is a consequence of elementary trigonometric identities. $\qquad\square$

In concrete terms, the result of Lemma 3.3 means

$$b_j(\boldsymbol{x}) = \begin{cases} \frac{1}{p}\sum_{k=1}^p e_k(\boldsymbol{x}) & \text{for } j = 1, \\ (\mathrm{i}\omega)^{-\frac{j}{2}}\frac{2}{p}\sum_{k=1}^p \cos(\frac{j}{2}\varphi_k)e_k(\boldsymbol{x}) & \text{for even } j, \\ (\mathrm{i}\omega)^{-\frac{j-1}{2}}\frac{2}{p}\sum_{k=1}^p \sin(\frac{j-1}{2}\varphi_k)e_k(\boldsymbol{x}) & \text{for odd } j \geq 3. \end{cases} \tag{3.17}$$

Remark 3.4. Use of the stable basis $\{b_j\}_{j=1}^p$ is essential in numerical studies of low-wavenumber asymptotics. Yet, the representation (3.17) is prone to cancellation and useless in numerical terms. Instead, we use the series expansion (3.12) up to ω^{13}. The resulting truncation errors are illustrated in Figure 1: for large ω the truncation error becomes large, for small ω the instability of the exponential basis makes the (MATLAB) computation sensitive to roundoff. For $\frac{1}{2} \leq \omega \leq 1$, $\boldsymbol{x} \in K$, and $p \leq 11$ the resulting truncation errors are below 10^{-5} uniformly.

Remark 3.5. The construction of a stable basis is closely linked to plane wave representation formulas for circular wave Helmholtz solutions

$$\boldsymbol{x} \mapsto \omega^{-n}J_n(\omega r)\exp(\pm \mathrm{i}n\theta), \quad \boldsymbol{x} = \begin{pmatrix} r\cos\theta \\ r\sin\theta \end{pmatrix}, \quad n \in \mathbb{N}_0, \tag{3.18}$$

where J_n is a Bessel function. For those we have the integral representation

$$J_n(z) = \frac{(-1)^n}{2\pi} \int_0^{2\pi} \exp(\mathrm{i} z \cos\varphi) \mathrm{e}^{\mathrm{i} n\varphi} \, \mathrm{d}\varphi, \quad z \in \mathbb{C}, \; n \in \mathbb{N}_0. \tag{3.19}$$

From the series expansion

$$J_n(z) = \left(\frac{z}{2}\right)^n \sum_{l=0}^{\infty} \frac{1}{l!(n+l)!} \left(-\frac{z^2}{4}\right)^l, \quad z \in \mathbb{C}, \tag{3.20}$$

it becomes clear that, in the limit $\omega \to 0$, the span of the functions, written in polar coordinates (r, θ),

$$\left\{ J_0(\omega r), \operatorname{Re} \frac{J_1(\omega r)}{\omega} \mathrm{e}^{\mathrm{i}\theta}, \operatorname{Im} \frac{J_1(\omega r)}{\omega} \mathrm{e}^{\mathrm{i}\theta}, \ldots, \operatorname{Re} \frac{J_m(\omega r)}{\omega^m} \mathrm{e}^{\mathrm{i} m\theta}, \operatorname{Im} \frac{J_m(\omega r)}{\omega^m} \mathrm{e}^{\mathrm{i} m\theta} \right\} \tag{3.21}$$

will be the same as that of the harmonic polynomials in (3.15). This suggests a relationship to the stable basis functions b_j from (3.4):

$$b_1 \sim J_0(\omega r), \quad b_j \sim \begin{cases} \omega^{-\frac{j}{2}} \operatorname{Re} J_{\frac{j}{2}}(\omega r) \mathrm{e}^{\mathrm{i}\frac{j}{2}\theta} & \text{for even } j, \\ \omega^{-\frac{j-1}{2}} \operatorname{Im} J_{\frac{j-1}{2}}(\omega r) \mathrm{e}^{\mathrm{i}\frac{j-1}{2}\theta} & \text{for odd } j. \end{cases} \tag{3.22}$$

Using (3.19) we can rewrite

$$J_n(\omega r) \mathrm{e}^{\mathrm{i} n\theta} = \frac{(-1)^n}{2\pi} \int_0^{2\pi} \exp(\mathrm{i} n\varphi) \exp\left(\mathrm{i}\omega \begin{pmatrix} \cos\varphi \\ \sin\varphi \end{pmatrix} \cdot \boldsymbol{x}\right) \mathrm{d}\varphi. \tag{3.23}$$

The integral can be approximated by the *p*-point trapezoidal rule, $p = 2m+1$. In combination with (3.22) this yields

$$b_1(\boldsymbol{x}) \sim \frac{1}{p} \sum_{l=1}^{p} \exp(\mathrm{i}\omega \boldsymbol{d}_l \cdot \boldsymbol{x}),$$

$$b_j(\boldsymbol{x}) \sim \begin{cases} \omega^{-\frac{j}{2}} \frac{1}{p} \sum_{l=1}^{p} \cos(\frac{j}{2}\varphi_l) e_l(\boldsymbol{x}) & \text{for even } j, \\ \omega^{-\frac{j-1}{2}} \frac{1}{p} \sum_{l=1}^{p} \sin(\frac{j-1}{2}\varphi_l) e_l(\boldsymbol{x}) & \text{for odd } j, \end{cases}$$

with $\boldsymbol{d}_l$ introduced in (3.16), φ_l defined in Lemma 3.3. Up to scaling this agrees with (3.17).

Some theoretical investigations will also rely on the augmented space

$$\begin{aligned} PPW_\omega(\mathbb{R}^2) &:= PW_\omega(\mathbb{R}^2) + \mathcal{P}_1(\mathbb{R}^2) \\ &= \langle 1, \mathrm{i}\omega x, \mathrm{i}\omega y, \exp(\mathrm{i}\omega \boldsymbol{d}_1 \cdot \boldsymbol{x}), \ldots, \exp(\mathrm{i}\omega \boldsymbol{d}_p \cdot \boldsymbol{x}) \rangle, \end{aligned} \tag{3.24}$$

where $\mathcal{P}_1(\mathbb{R}^2)$ designates the space of two-variate affine linear functions. For theoretical purposes we also need a basis of $PPW_\omega(\mathbb{R}^2)$ that remains stable for $\omega \to 0$. Its construction is guided by the very same ideas as that of the stable basis $\{b_1, \ldots, b_p\}$ of $PW_\omega(\mathbb{R}^2)$. For details we refer to Section 4 of the technical report [18].

3.2. **Inverse and projection estimates for plane waves**

In order to develop a convergence theory for the *h*-version of the DG methods from Section 2 with plane wave trial and test functions, we aim to establish element-by-element inverse and projection estimates for $PW_\omega^{p,\xi}(\mathbb{R}^2)$ that parallel those for piecewise polynomials. As usual we have to limit the distortion of the triangles.

Assumption 3.6 (shape regularity). *All angles of triangles in $\mathcal{T}_h$ are bounded from below by $\alpha_0 > 0$.*

Our analysis heavily relies on *scaling techniques* employing similarity mappings $\mathbf{\Phi}_K$, that is, compositions of rigid motions and scalings:

$$\mathbf{\Phi}_K : \widehat{K} \mapsto K, \quad \mathbf{\Phi}_K(\widehat{\boldsymbol{x}}) = \tfrac{h_K}{h_{\widehat{K}}}\, \mathbf{Q}\widehat{\boldsymbol{x}} + \boldsymbol{t}, \ \ \mathbf{Q}^T = \mathbf{Q}^{-1}, \ \boldsymbol{t} \in \mathbb{R}^2, \tag{3.25}$$

where $\widehat{K}$ is another triangle of the same shape. A function $v \in PW_\omega^{p,0}(K)$ pulled back to $\widehat{K}$ has the representation

$$(v \circ \mathbf{\Phi}_K)(\widehat{\boldsymbol{x}}) =: \widehat{v}(\widehat{\boldsymbol{x}}) = \sum_{j=1}^p \alpha_j \exp(\mathrm{i}\, \tfrac{h_K}{h_{\widehat{K}}}\, \omega \widehat{\boldsymbol{d}}_j \cdot \widehat{\boldsymbol{x}}), \quad \alpha_j \in \mathbb{C}, \ \widehat{\boldsymbol{x}} \in \widehat{K}, \tag{3.26}$$

with, by (3.16),

$$\widehat{\boldsymbol{d}}_j = \begin{pmatrix} \cos(\tfrac{2\pi}{p}(j-1) + \gamma) \\ \sin(\tfrac{2\pi}{p}(j-1) + \gamma) \end{pmatrix}, \quad j = 1, \ldots, p, \quad \gamma \in \mathbb{R}. \tag{3.27}$$

The angle γ reflects the rotation $\mathbf{Q}$ involved in the mapping to $\widehat{K}$. In short, the image of $PW_\omega^{p,0}(\mathbb{R}^2)$ under similarity pullback is $PW_{\widehat{\omega}}^{p,\gamma}(\mathbb{R}^2)$, $\widehat{\omega} := \tfrac{h_K}{h_{\widehat{K}}}\, \omega$. It is essential to note that even if two triangles are mapped to the same "reference triangle" $\widehat{K}$, the mapped plane wave spaces will not necessarily agree. This foils standard finite element Bramble-Hilbert type arguments, see [6], Section 4.3.8.

The first class of inequalities are trace inverse estimates connecting norms of traces onto element boundaries with norms over the element itself.

Theorem 3.7. *Let Assumption 3.6 hold and p be odd. Then there exists a constant $C_{\mathrm{tinv}} > 0$ such that*

$$\|v\|_{0,\partial K} \leq C_{\mathrm{tinv}} h_K^{-1/2} \|v\|_{0,K} \qquad \forall v \in PW_\omega^{p,0}(\mathbb{R}^2), \ \forall K \in \mathcal{T}_h, \ \forall \omega \geq 0.$$

Proof. (*i*) Pick any $K \in \mathcal{T}_h$ and an edge $e \subset \partial K$. There is a unique similarity mapping $\mathbf{\Phi}_K$ according to (3.25) such that the line segment $\widehat{e} = \left[\binom{-1}{0}, \binom{1}{0} \right]$ is mapped onto e. Write $\widehat{K}$ for the pre-image of K under $\mathbf{\Phi}_K$. If we can establish the existence of $C > 0$ that may only depend on α_0 from Assumption 3.6, such that

$$\|v\|_{0,\widehat{e}} \leq C \|v\|_{0,\widehat{K}} \quad \forall v \in PW_{\widehat{\omega}}^{p,\gamma}(\mathbb{R}^2), \ \forall \gamma \in [0, 2\pi[, \ \forall \widehat{\omega} \in \mathbb{R}^+, \tag{3.28}$$

then the assertion of the theorem will follow by simple scaling arguments. Assumption 3.6 also guarantees that the isoceles triangle T with base $\widehat{e}$ and base angle α_0 is contained in $\widehat{K}$. Thus, (3.28) is already implied by

$$\exists C > 0 : \quad \|v\|_{0,\widehat{e}} \leq C \|v\|_{0,T} \quad \forall v \in PW_{\widehat{\omega}}^{p,\gamma}(\mathbb{R}^2), \ \forall \gamma \in [0, 2\pi[, \ \forall \widehat{\omega} \in \mathbb{R}^+. \tag{3.29}$$

(*ii*) If we choose some basis $\{w_j\}_{j=1}^p$ of $PW_{\widehat{\omega}}^{p,\gamma}(\mathbb{R}^2)$, the computation of the best possible value for C from (3.29) can be converted into a generalized eigenvalue problem for matrices: this C agrees with the square root of the largest eigenvalue $\lambda_{\max} = \lambda_{\max}(\widehat{\omega}, \gamma)$ of the generalized eigenvalue problem

$$\lambda \in \mathbb{R}, \ \vec{\alpha} \in \mathbb{R}^p \setminus \{0\} : \quad \boldsymbol{T}\vec{\alpha} = \lambda \boldsymbol{M}\vec{\alpha}, \tag{3.30}$$

with the mass matrices

$$\boldsymbol{T} := \left(\int_{\widehat{e}} w_k(\boldsymbol{x}) \cdot \overline{w}_j(\boldsymbol{x}) \, \mathrm{d}S \right)_{1 \le k,j \le p}, \quad \boldsymbol{M} := \left(\int_{T} w_k(\boldsymbol{x}) \cdot \overline{w}_j(\boldsymbol{x}) \, \mathrm{d}\boldsymbol{x} \right)_{1 \le k,j \le p}.$$

The eigenvalues of (3.30) do not depend on the choice of basis. Guided by convenience, we may therefore either choose the stable basis $\{b_j\}_{j=1}^p$ from (3.17) or the standard basis $\{e_j\}_{j=1}^p$.

(*iii*) No matter which basis is used, both Hermitian $p \times p$-matrices $\boldsymbol{T}$ and $\boldsymbol{M}$ are continuous functions of $\widehat{\omega} \in \mathbb{R}^+$, $\gamma \in [0, 2\pi]$. Moreover, linear independence of the plane waves renders $\boldsymbol{M}$ positive definite for $\widehat{\omega} \neq 0$. Hence, the eigenvalues will be continuous functions of $\widehat{\omega}$ and γ on $\mathbb{R}^+ \times [0, 2\pi]$ (and periodic in γ).

For small ω, the basis $\{b_j\}_{j=1}^p$ is convenient. The uniform convergence of the b_j for $\widehat{\omega} \to 0$ carries over to the mass matrices. Both $\boldsymbol{T}$ and $\boldsymbol{M}$ enjoy a uniform limit for $\widehat{\omega} \to 0$, which agrees with the mass matrices $\boldsymbol{T}^0$, $\boldsymbol{M}^0$ arising from the use of the harmonic polynomial basis $\{b_j^0\}_{j=1}^p$, see (3.15). Obviously, $\boldsymbol{M}^0$ is positive definite, and $\boldsymbol{T}^0$ does not vanish. Hence, the eigenvalues from (3.30) (as functions of $\widehat{\omega}$) have a continuous extension to $\widehat{\omega} = 0$. Note that the limit does not depend on γ.

We conclude, that $\lambda_{\max}(\widehat{\omega}, \gamma)$ can be extended to $\widehat{\omega} = 0$ with a positive value $\lambda_{\max}(0, \gamma) = \lambda_{\max}(0) > 0$ (independent of γ). Thus, $\lambda_{\max}$ turns out to be a positive and continuous function on $\mathbb{R}_0^+ \times [0, 2\pi]$.

(*iv*) To determine the behavior of $\lambda_{\max}(\widehat{\omega}, \gamma)$ for $\widehat{\omega} \to \infty$, we resort to the standard basis $\{e_k\}_{k=1}^p$. Then, writing $\delta x_{jk} := d_{j,1} - d_{k,1}$, $\delta y_{jk} := d_{j,2} - d_{k,2}$, $a := \tan(\alpha_0)$, we find

$$(\boldsymbol{T})_{jk} = 2 \operatorname{sinc}(\mathrm{i}\widehat{\omega}\delta x_{jk}), \quad 1 \le k, j \le p, \tag{3.31}$$

$$(\boldsymbol{M})_{jk} = \int_0^a \int_{-1+y/a}^{1-y/a} \exp(\mathrm{i}\widehat{\omega}(\delta x_{jk}x + \delta y_{jk}y)) \, \mathrm{d}x \, \mathrm{d}y, \quad 1 \le k, j \le p. \tag{3.32}$$

Obviously, the Euclidean matrix norm of $\boldsymbol{T}$ can be bounded by $\|\boldsymbol{T}\| \le 2p$. Further, $\boldsymbol{M}_{jj} = a$ for $1 \le j \le p$. To estimate the off-diagonal matrix entries $(\boldsymbol{M})_{jk}$, $k \neq j$, we use $|\boldsymbol{d}_j - \boldsymbol{d}_k|^2 = \delta x_{kj}^2 + \delta y_{kj}^2 = 4\sin^2(\frac{\pi}{p}|k - j|)$ and distinguish two cases.

(*a*) If $|\delta x_{jk}| \ge |\delta y_{jk}|$, we infer $|\delta x_{jk}| \ge \sin(\frac{\pi}{p}|k - j|) > 0$. Thus, we can directly evaluate the inner integral of (3.32)

$$(\boldsymbol{M})_{jk} = 2 \int_0^a \exp(\mathrm{i}\widehat{\omega}\delta y_{jk}y)(1 - y/a) \operatorname{sinc}(\widehat{\omega}\delta x_{jk}(1 - y/a)) \, \mathrm{d}y$$

$$\le 2a \int_0^1 \min\left\{1 - y, \frac{1}{\widehat{\omega}\delta x_{jk}}\right\} \, \mathrm{d}y = \frac{a}{\widehat{\omega}\delta x_{jk}} \left(1 + \frac{1}{\widehat{\omega}\delta x_{jk}} - \frac{1}{(\widehat{\omega}\delta x_{jk})^2}\right).$$

This expression tends to zero uniformly as $\widehat{\omega} \to \infty$.

(*b*) In the case $|\delta x_{jk}| < |\delta y_{jk}|$, that is, $|\delta y_{jk}| > \sin(\frac{\pi}{p}|k - j|) > 0$, we change the order of integration in (3.32) and obtain

$$(\boldsymbol{M})_{jk} = 2 \int_0^1 \cos(\widehat{\omega}\delta x_{jk}x) \frac{\exp(\mathrm{i}\widehat{\omega}\delta y_{jk}a(1 - x)) - 1}{\mathrm{i}\widehat{\omega}\delta y_{jk}} \, \mathrm{d}x$$

$$\le 4 \int_0^1 \min\left\{a(1 - x), \frac{1}{\widehat{\omega}\delta y_{jk}}\right\} \, \mathrm{d}y \to 0 \text{ uniformly as } \widehat{\omega} \to \infty.$$
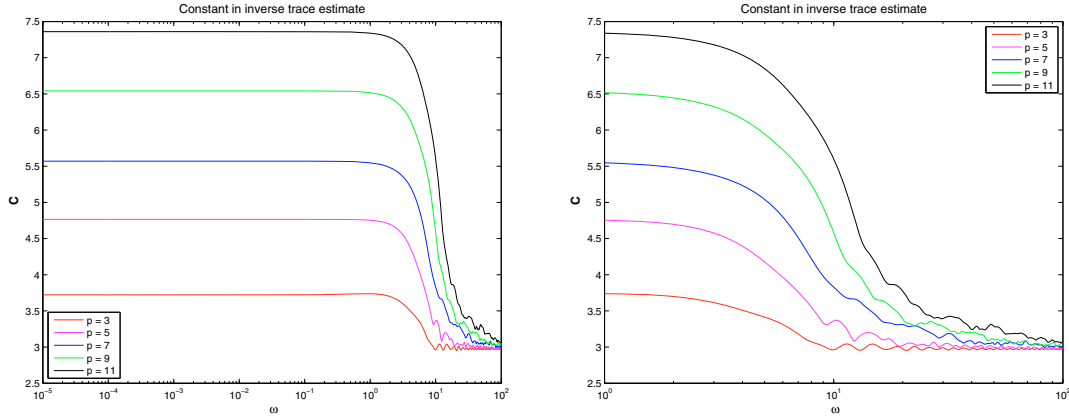
FIGURE 2. Constants in the inverse trace norm inequality of Theorem 3.7 for the unit triangle.

Summing up, we found the asymptotic behavior

$$\max_{\substack{1 \leq i,j \leq p \\ j \neq k}} (\boldsymbol{M})_{i,j} = O(\widehat{\omega}^{-1}) \quad \text{for } \widehat{\omega} \to \infty. \tag{3.33}$$

As a consequence, for $\widehat{\omega}$ large enough, Gershgorin's theorem tells us that the smallest eigenvalue of $\boldsymbol{M}$ can be bounded from below by $\frac{1}{2}a$. We immediately infer

$$\lim_{\widehat{\omega} \to \infty} \lambda_{\max}(\widehat{\omega}, \gamma) \leq \lim_{\widehat{\omega} \to \infty} \lambda_{\min}(\boldsymbol{M})^{-1} \|\boldsymbol{T}\| \leq \frac{4p}{a} \qquad \forall \gamma \in [0, 2\pi[. \tag{3.34}$$

Summing up, $\lambda_{\max}(\widehat{\omega}, \gamma)$ is bounded on $\mathbb{R}_0^+ \times [0, 2\pi]$, which ensures the existence of a $C_{\text{tinv}} > 0$ in (3.29). $\square$

Numerical experiment. We have computed the constant in the inverse estimate of Theorem 3.7 numerically for the "unit triangle" $K := \{\boldsymbol{x} \in \mathbb{R}^2 : x_1, x_2 > 0, \ x_1 + x_2 < 1\}$, see Figure 2. In addition, the shape of the triangle $K := \{\boldsymbol{x} \in \mathbb{R}^2 : x_1, x_2 > 0, \ ax_1 + x_2 < a\}$ is varied smoothly in Figure 3. The computation were carried out in MATLAB using the standard exponential basis $\{e_k\}$ of PW_ω for $\omega \geq \frac{1}{2}$. For smaller ω the computations employed the first 13 terms in the Taylor expansions (w.r.t. ω) of the stable basis functions b_j from (3.4).

The plots strikingly illustrate the uniform boundedness of the constant in the inverse trace inequality with respect to ω. Smooth dependence on the geometry of K is also apparent. The bound for the constants is moderate, but seems to increase linearly with p. Remember that this is also true for multivariate polynomials of degree p; see, *e.g.*, [31], Theorem 4.76.

Theorem 3.8. *There exists a constant $C_{\text{inv}} > 0$ only depending on p and α_0 such that*

$$\|\nabla v\|_{0,K} \leq C_{\text{inv}}(\omega h_K + 1) \, h_K^{-1} \|v\|_{0,K} \quad \forall v \in PW_\omega^{p,0}(\mathbb{R}^2), \ \forall K \in \mathcal{T}_h, \ \forall \omega \geq 0.$$

Proof. Again we resort to transformation techniques and first establish the estimate for the reference triangle $\widehat{K}$. Thanks to integration by parts and Theorem 3.7 (recall that plane wave spaces are invariant with respect to forming partial derivatives), we have

$$\int_{\widehat{K}} |\nabla \widehat{v}|^2 \, \mathrm{d}\widehat{\boldsymbol{x}} = -\int_{\widehat{K}} \Delta \widehat{v} \cdot \bar{\widehat{v}} \, \mathrm{d}\widehat{\boldsymbol{x}} + \int_{\partial \widehat{K}} \nabla \widehat{v} \cdot \widehat{\boldsymbol{n}} \, \bar{\widehat{v}} \, \mathrm{d}\widehat{S} \leq \widehat{\omega}^2 \int_{\widehat{K}} |\widehat{v}|^2 \, \mathrm{d}\widehat{\boldsymbol{x}} + \|\nabla \widehat{v}\|_{0,\partial \widehat{K}} \|\widehat{v}\|_{0,\partial \widehat{K}}$$

$$\leq \widehat{\omega}^2 \|\widehat{v}\|_{0,\widehat{K}}^2 + C_{\text{tinv}}^2 \|\nabla \widehat{v}\|_{0,\widehat{K}} \|\widehat{v}\|_{0,\widehat{K}} \leq \left(\widehat{\omega}^2 + \tfrac{1}{2} C_{\text{tinv}}^4\right) \|\widehat{v}\|_{0,\widehat{K}}^2 + \frac{1}{2} \|\nabla \widehat{v}\|_{0,\widehat{K}}^2.$$
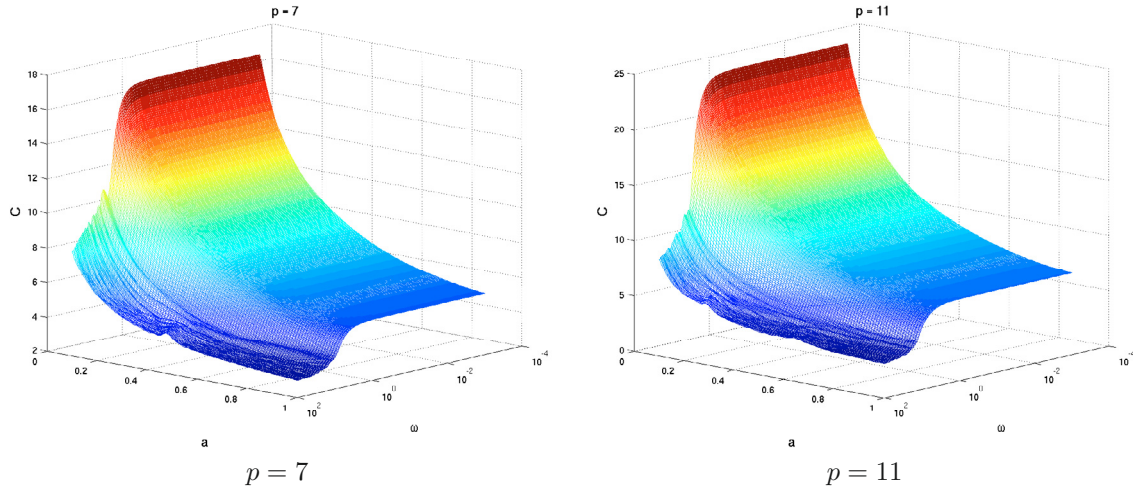
Then transform this estimate to K. $\square$

$$p = 7 \qquad\qquad p = 11$$

FIGURE 3. Constants in the inverse trace norm inequality for triangle with vertices $\binom{0}{0}, \binom{1}{0}, \binom{0}{a}$, $a > 0$.
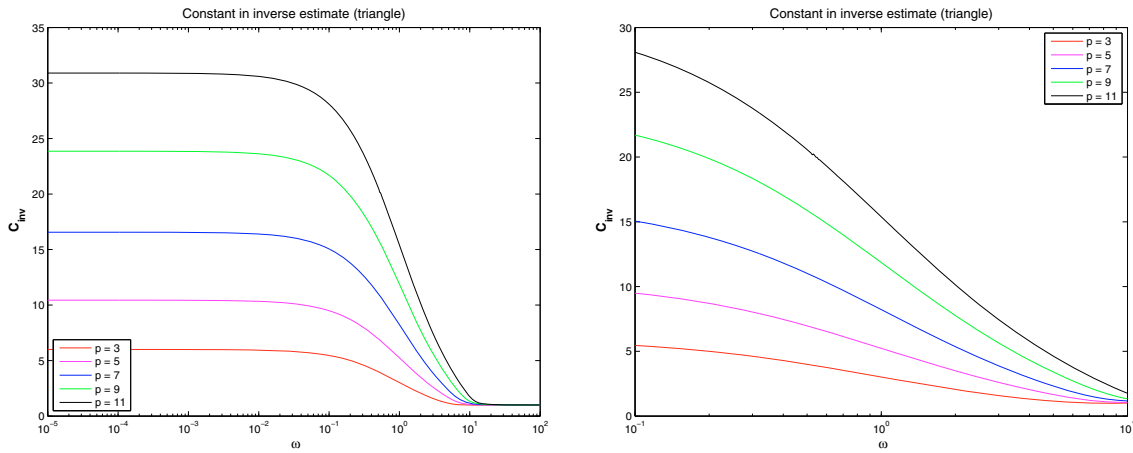

FIGURE 4. Constant in inverse inequality of Theorem 3.8 for the unit triangle.

Numerical experiment. Figure 4 displays approximate values for C_{inv} from Theorem 3.8 for the "unit triangle" $K := \{ \boldsymbol{x} \in \mathbb{R}^2 : x_1, x_2 > 0,\ x_1 + x_2 < 1 \}$ ($h_K = 1$ in each case). The computations were done in MATLAB and used the truncated stable basis for $\omega \le \frac{1}{2}$, see the previous numerical experiments.

Proposition 3.9. *The estimates of Theorems 3.7 and 3.8 still hold with $PW_\omega^{p,\gamma}(\mathbb{R}^2)$ replaced by $PPW_\omega^{p,\gamma}(\mathbb{R}^2)$.*

Proof. The proof can be done as above, because a basis of $PPW_\omega^{p,\gamma}(\mathbb{R}^2)$ that remains stable for $\omega \to 0$ is available. ∎

Next, we examine approximation and projection estimates for plane waves. We fix a triangle K that complies with Assumption 3.6. We study the local $L^2(K)$-orthogonal projections

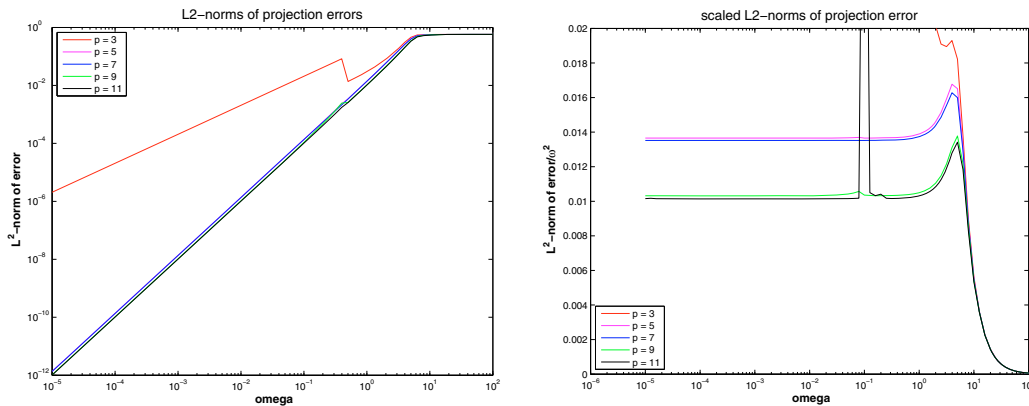$$\mathsf{P}_\omega : L^2(K) \mapsto PW_\omega^{p,\gamma}(\mathbb{R}^2) \tag{3.35}$$

FIGURE 5. $L^2(]0,1[^2)$ projection error onto plane wave space for linear function $\boldsymbol{x} \mapsto x$. The wiggles at $\omega = \frac{1}{2}$ are due to the truncation error for the stable basis.

onto the space of plane waves on K, see (3.16). When referring to the associated reference element $\widehat{K}$ with longest edge $\left[\binom{0}{0}, \binom{1}{0}\right]$ and the pulled back plane wave space we write $\widehat{\mathsf{P}}_{\widehat{\omega}}$ for this projector.

We pursue the policy to relate P_ω to the $L^2(K)$-orthogonal projection $\mathsf{Q} : L^2(K) \mapsto \mathcal{P}_1(\mathbb{R}^2)$ onto the space of bi-variate polynomials of degree 1. Simple transformation techniques and Bramble-Hilbert arguments establish the projection error estimates

$$
\begin{aligned}
\|u - \mathsf{Q}u\|_{0,K} &\leq Ch_K^2 |u|_{2,K} \\
|u - \mathsf{Q}u|_{1,K} &\leq Ch_K |u|_{2,K}
\end{aligned}
\quad \forall u \in H^2(K), \tag{3.36}
$$

with $C > 0$ only depending on the minimal angle condition in Assumption 3.6.

The next Lemma gives a pivotal auxiliary result.

Lemma 3.10. *For odd $p \geq 5$ we find $C > 0$ independent of ω and γ (but, of course, depending on p) such that*

$$
\inf_{v \in PW_\omega^{p,\gamma}(\mathbb{R}^2)} \|q - v\|_{0,]0,1[^2} \leq C\omega^2 \|q\|_{0,]0,1[^2} \quad \forall q \in \mathcal{P}_1(\mathbb{R}^2).
$$

Proof. Recall (3.10), the definition of $\kappa_j^n(\boldsymbol{x})$ and the formula (3.12) for the functions of the stabilized basis. Combining them, we see that, for $p \geq 5$ and $\omega \to 0$,

$$
b_1(\boldsymbol{x}) = 1 + O(\omega^2), \quad b_2(\boldsymbol{x}) = x + O(\omega^2), \quad b_3(\boldsymbol{x}) = y + O(\omega^2),
$$

for small ω uniformly in $\boldsymbol{x} \in]0,1[^2$ and $\gamma \in [0, 2\pi[$.

It goes without saying that the assertion needs only be shown for $q(\boldsymbol{x}) = 1$, $q(\boldsymbol{x}) = x$, and $q(\boldsymbol{x}) = y$. Then choose b_1, b_2, and b_3, respectively, as approximating plane wave functions. $\square$

Remark 3.11. In the case $p = 3$ the best approximation error for linear functions will behave like $O(\omega)$, because it will be affected by the remainder term in (3.13).

Numerical experiment. We computed the error of the L^2-projection of the function $\boldsymbol{x} \mapsto x$ onto the plane wave space on $]0,1[^2$ numerically, see Figure 5. As above, a truncated stable basis and the exponential basis were used for $\omega < \frac{1}{2}$ and $\omega \geq \frac{1}{2}$, respectively. The measured errors are in perfect agreement with Lemma 3.10, but also shows that the estimate in Lemma 3.10 is sharp and the constants are small.

In the next three propositions we establish projection errors and continuity of the $L^2(K)$-orthogonal projection P_ω onto $PW_\omega^{p,0}(\mathbb{R}^2)$.

Proposition 3.12. *For odd $p \geq 5$ we have, with $C = C(p, \alpha_0) > 0$ independent of K and $\omega \geq 0$,*

$$\|(Id - \mathsf{P}_\omega)u\|_{0,K} \leq Ch_K^2(|u|_{2,K} + \omega^2\|u\|_{0,K}) \quad \forall u \in H^2(K).$$

Proof. Again, we use scaling arguments: consider the reference element $\widehat{K} \subset]0, 1[^2$. First of all, from Lemma 3.10, the equivalence of all norms on $\mathcal{P}_1(\mathbb{R}^2)$ and continuity of the $L^2(\widehat{K})$-projection onto $\mathcal{P}_1(\mathbb{R}^2)$, we obtain the estimate

$$\|(Id - \widehat{\mathsf{P}}_{\widehat{\omega}})\widehat{\mathsf{Q}}\widehat{u}\|_{0,\widehat{K}} \leq C\widehat{\omega}^2\|\widehat{\mathsf{Q}}\widehat{u}\|_{0,]0,1[^2} \leq C\widehat{\omega}^2\|\widehat{\mathsf{Q}}\widehat{u}\|_{0,\widehat{K}} \leq C\widehat{\omega}^2\|\widehat{u}\|_{0,\widehat{K}} \quad \forall u \in H^2(K), \tag{3.37}$$

with a constant $C > 0$ independent of $\widehat{\omega}$. Then, by the triangle inequality, we get

$$\|(Id - \widehat{\mathsf{P}}_{\widehat{\omega}})\widehat{u}\|_{0,\widehat{K}} \leq \|(Id - \widehat{\mathsf{P}}_{\widehat{\omega}}\widehat{\mathsf{Q}})\widehat{u}\|_{0,\widehat{K}} \leq \|\widehat{u} - \widehat{\mathsf{Q}}\widehat{u}\|_{0,\widehat{K}} + \|(Id - \widehat{\mathsf{P}}_{\widehat{\omega}})\widehat{\mathsf{Q}}\widehat{u}\|_{0,\widehat{K}}$$

$$\overset{\text{proj. est.}}{\leq} C\,|\widehat{u}|_{2,\widehat{K}} + \|(Id - \widehat{\mathsf{P}}_{\widehat{\omega}})\widehat{\mathsf{Q}}\widehat{u}\|_{0,\widehat{K}} \overset{(3.37)}{\leq} C\,|\widehat{u}|_{2,\widehat{K}} + C\widehat{\omega}^2\|\widehat{u}\|_{0,\widehat{K}}.$$

Now, taking into account that transformation to the reference element changes the frequency according to $\widehat{\omega} = h_K\omega$, the result is an immediate consequence of norm transformation estimates. $\square$

Proposition 3.13. *For odd $p \geq 5$ we have, with $C = C(p, \alpha_0) > 0$ independent of K and $\omega \geq 0$*

$$|(Id - \mathsf{P}_\omega)u|_{1,K} \leq Ch_K(\omega h_K + 1)(|u|_{2,K} + \omega^2\|u\|_{0,K}) \quad \forall u \in H^2(K).$$

Proof. By the triangle inequality we have

$$|(Id - \mathsf{P}_\omega)u|_{1,K} \leq |u - \mathsf{Q}u|_{1,K} + |(Id - \mathsf{P}_\omega)\mathsf{Q}u|_{1,K} + |\mathsf{P}_\omega(\mathsf{Q}u - u)|_{1,K}. \tag{3.38}$$

Owing to (3.36), for the first term we get

$$|u - \mathsf{Q}u|_{1,K} \leq Ch_K|u|_{2,K}, \tag{3.39}$$

with $C > 0$ independent of K and, obviously, of ω. To tackle second term we appeal to Proposition 3.9 and use transformation to the reference triangle $\widehat{K}$

$$|(Id - \mathsf{P}_\omega)\mathsf{Q}u|_{1,K} = |(Id - \widehat{\mathsf{P}}_{\widehat{\omega}})\widehat{\mathsf{Q}}\widehat{u}|_{1,\widehat{K}} \leq |(Id - \widehat{\mathsf{P}}_{\widehat{\omega}})\widehat{\mathsf{Q}}\widehat{u}|_{1,]0,1[^2} \overset{\text{Prop. 3.9}}{\leq} C(1 + \widehat{\omega})\|(Id - \widehat{\mathsf{P}}_{\widehat{\omega}})\widehat{\mathsf{Q}}\widehat{u}\|_{0,]0,1[^2}$$

$$\overset{\text{Lem. 3.10}}{\leq} C(1 + \widehat{\omega})\widehat{\omega}^2\|\widehat{\mathsf{Q}}u\|_{0,]0,1[^2} \overset{(*)}{\leq} C(1 + \widehat{\omega})\widehat{\omega}^2\|\widehat{\mathsf{Q}}u\|_{0,\widehat{K}}$$

$$\leq C(1 + \widehat{\omega})\widehat{\omega}^2\|u\|_{0,\widehat{K}} \leq C(1 + h_K\omega)\omega^2 h_K\|u\|_{0,K} \tag{3.40}$$

again with $C > 0$ independent of K and ω. Step $(*)$ appeals to the equivalence of the L^2-norms of affine linear functions on different compact sets. The last step relies on the transformation of L^2-norm under scaling and uses $\widehat{\omega} = h_K\omega$.

Eventually, the third term allows the bounds

$$|\mathsf{P}_\omega(\mathsf{Q}u - u)|_{1,K} \overset{\text{Thm. 3.8}}{\leq} C(\omega h_K + 1)h_K^{-1}\|\mathsf{P}_\omega(\mathsf{Q}u - u)\|_{0,K}$$

$$\overset{\text{cont. of } \mathsf{P}_\omega}{\leq} C(\omega h_K + 1)h_K^{-1}\|\mathsf{Q}u - u\|_{0,K} \overset{\text{proj. est.}}{\leq} C(\omega h_K^2 + h_K)|u|_{2,K}. \tag{3.41}$$

Also in this case the constants can be chosen independently of K and ω. Inserting (3.39)–(3.41) into (3.38) gives the assertion. $\square$

Proposition 3.14. *For odd $p \geq 5$ we have, with $C = C(p, \alpha_0) > 0$ independent of K and $\omega \geq 0$,*

$$|\mathsf{P}_\omega u|_{2,K} \leq C(\omega h_K + 1)^2 \big(|u|_{2,K} + \omega^2 \|u\|_{0,K}\big) \quad \forall u \in H^2(K).$$

Proof. Since the second derivatives of $\mathsf{Q}u$ vanish, the triangle inequality gives

$$|\mathsf{P}_\omega u|_{2,K} \leq |\mathsf{P}_\omega(u - \mathsf{Q}u)|_{2,K} + |(\mathsf{P}_\omega - Id)\mathsf{Q}u|_{2,K}. \tag{3.42}$$

Since $PW_\omega^{p,0}$ is invariant w.r.t. forming partial derivatives, we have

$$|\mathsf{P}_\omega(u - \mathsf{Q}u)|_{2,K} \overset{\text{Thm. 3.8}}{\leq} C_{\text{inv}}(\omega h_K + 1)h_K^{-1}|\mathsf{P}_\omega(u - \mathsf{Q}u)|_{1,K} \overset{(3.41)}{\leq} C(\omega h_K + 1)^2|u|_{2,K}, \tag{3.43}$$

with $C > 0$ independent of h_K and ω, and

$$
\begin{aligned}
|(\mathsf{P}_\omega - Id)\mathsf{Q}u|_{2,K} &\overset{\text{Prop. 3.9}}{\leq} && C(\omega h_K + 1)h_K^{-1}|(\mathsf{P}_\omega - Id)\mathsf{Q}u|_{1,K} \\
&\overset{(??)}{\leq} && C(\omega h_K + 1)h_K^{-1}(\omega^3 h_K^2 + \omega^2 h_K)\|u\|_{0,K} \\
&= && C(\omega h_K + 1)(\omega^3 h_K + \omega^2)\|u\|_{0,K},
\end{aligned} \tag{3.44}
$$

again with $C > 0$ independent of h_K and ω. Inserting (3.43) and (3.44) into (3.42) gives the result. $\qquad \square$

4. Convergence analysis

Duality arguments are the linchpin of our analysis, and, inevitably, they hinge on elliptic lifting estimates for the Helmholtz operator, *cf.* [6], Section 5.8. Thus, from now on, we assume that Ω is a *convex* polygon. We also recall that $\mathcal{T}_h$ is a triangular mesh with possible hanging nodes satisfying Assumption 3.6.

Set

$$V_h = \{v \in L^2(\Omega) \ : \ v_{|_K} \in PW_\omega^{p,0}(\mathbb{R}^2) \ \forall K \in \mathcal{T}_h\}, \tag{4.1}$$

and let $V \subseteq H^2(\Omega)$ be the space containing all possible u such that $-\Delta u - \omega^2 u \in L^2(\Omega)$ and $\nabla u \cdot \boldsymbol{n} + \mathrm{i}\omega\, u \in L^2(\partial\Omega)$.

In this section, we study the convergence of the method introduced in Section 2, with V_h as trial and test space. To this end, consider formulation (2.5), which is equivalent to (2.7) for our choice of V_h, with numerical fluxes given by (2.8) and (2.9).

Adding (2.5) over all elements and expanding the expressions of the numerical fluxes, with α as in (2.13) (we keep general β and δ, for the moment), we can write the primal DG method as follows: find $u_h \in V_h$ such that, for all $v_h \in V_h$,

$$a_h(u_h, v_h) - \omega^2(u_h, v_h) = (f, v_h) - \int_{\mathcal{F}_h^{\mathcal{B}}} \delta\, \frac{1}{\mathrm{i}\omega}\, g\, \overline{\nabla_h v_h \cdot \boldsymbol{n}}\, \mathrm{d}S + \int_{\mathcal{F}_h^{\mathcal{B}}} (1 - \delta)\, g\, \overline{v}_h\, \mathrm{d}S, \tag{4.2}$$

where $a_h(\cdot, \cdot)$ is the DG-bilinear form on $(V + V_h) \times (V + V_h)$ defined by

$$
\begin{aligned}
a_h(u, v) = {}& (\nabla_h u, \nabla_h v) - \int_{\mathcal{F}_h^{\mathcal{I}}} [\![u]\!]_N \cdot \{\!\!\{\overline{\nabla_h v}\}\!\!\}\, \mathrm{d}S - \int_{\mathcal{F}_h^{\mathcal{I}}} \{\!\!\{\nabla_h u\}\!\!\} \cdot [\![\overline{v}]\!]_N\, \mathrm{d}S \\
& - \int_{\mathcal{F}_h^{\mathcal{B}}} \delta\, u\, \overline{\nabla_h v \cdot \boldsymbol{n}}\, \mathrm{d}S - \int_{\mathcal{F}_h^{\mathcal{B}}} \delta\, \nabla_h u \cdot \boldsymbol{n}\, \overline{v}\, \mathrm{d}S \\
& - \frac{1}{\mathrm{i}\omega} \int_{\mathcal{F}_h^{\mathcal{I}}} \beta [\![\nabla_h u]\!]_N [\![\overline{\nabla_h v}]\!]_N\, \mathrm{d}S - \frac{1}{\mathrm{i}\omega} \int_{\mathcal{F}_h^{\mathcal{B}}} \delta\, \nabla_h u \cdot \boldsymbol{n}\, \overline{\nabla_h v \cdot \boldsymbol{n}}\, \mathrm{d}S \\
& + \mathrm{i} \int_{\mathcal{F}_h^{\mathcal{I}}} \frac{\mathsf{a}}{\mathsf{h}}\, [\![u]\!]_N \cdot [\![\overline{v}]\!]_N\, \mathrm{d}S + \mathrm{i}\omega \int_{\mathcal{F}_h^{\mathcal{B}}} (1 - \delta)\, u\, \overline{v}\, \mathrm{d}S.
\end{aligned} \tag{4.3}
$$

Proposition 4.1. *If $\beta > 0$, $0 < \delta < 1$, and $\mathtt{a}$ is uniformly positive, the discrete variational problem* (4.2) *possesses a unique solution for any $f \in L^2(\Omega)$ and $g \in L^2(\partial\Omega)$.*

Proof. Note that $\mathrm{Im}\,(a_h(v_h, v_h)) > 0$ for all $v_h \in V_h$. $\square$

The DG method (4.2) is consistent by construction, and thus, if u is the analytical solution of (1.1),

$$a_h(u - u_h, v_h) = \omega^2(u - u_h, v_h) \qquad \forall v_h \in V_h. \tag{4.4}$$

Taking the cue from the definition of $a_h(\cdot, \cdot)$, we define the following mesh-dependent seminorm and norms on $V + V_h$:

$$\begin{aligned}
|v|_{DG}^2 &:= \|\nabla_h v\|_{0,\Omega}^2 + \omega^{-1}\|\beta^{1/2}[\![\nabla_h v]\!]_N\|_{0,\mathcal{F}_h^{\mathcal{I}}}^2 + \|\mathtt{a}^{1/2}\mathtt{h}^{-1/2}[\![v]\!]_N\|_{0,\mathcal{F}_h^{\mathcal{I}}}^2 \\
&\quad + \omega^{-1}\|\delta^{1/2}\nabla_h v \cdot \boldsymbol{n}\|_{0,\mathcal{F}_h^{\mathcal{B}}}^2 + \omega\|(1-\delta)^{1/2}v\|_{0,\mathcal{F}_h^{\mathcal{B}}}^2, \\
\|v\|_{DG}^2 &:= |v|_{DG}^2 + \omega^2\|v\|_{0,\Omega}^2, \\
\|v\|_{DG+}^2 &:= \|v\|_{DG}^2 + \omega\|\beta^{-1/2}\{\!\!\{v\}\!\!\}\|_{0,\mathcal{F}_h^{\mathcal{I}}}^2 + \|\mathtt{a}^{-1/2}\mathtt{h}^{1/2}\{\!\!\{\nabla_h v\}\!\!\}\|_{0,\mathcal{F}_h^{\mathcal{I}}}^2 + \omega\|\delta^{-1/2}v\|_{0,\mathcal{F}_h^{\mathcal{B}}}^2.
\end{aligned}$$

We prove that the auxiliary DG-bilinear form, which is related to the positive operator $-\Delta + \omega^2$,

$$b_h(u, v) := a_h(u, v) + \omega^2(u, v)$$

is coercive in the DG-norm. To this end, we apply the inverse inequality for plane waves asserted in Theorem 3.7.

Proposition 4.2. *With the particular choice of $\alpha = \mathtt{a}/\omega\mathtt{h}$ (see* (2.13)*), with $\mathtt{a} \geq \mathtt{a}_{\min} > C_{\mathrm{tinv}}^2$ (C_{tinv} introduced in Thm.* 3.7*), and $0 < \delta < 1/2$ in the numerical fluxes* (2.8) *and* (2.9)*, there exists a constant $C_{\mathrm{coer}} > 0$ only depending on α_0 from Assumption* 3.6 *and on p, in particular, independent of ω and of the mesh, such that*

$$|b_h(v, v)| \geq C_{\mathrm{coer}}\|v\|_{DG}^2 \qquad \forall v \in V_h.$$

Proof. By definition, we have

$$\begin{aligned}
b_h(v, v) &= \|\nabla_h u\|_{0,\Omega}^2 - 2\,\mathrm{Re}\,\left(\int_{\mathcal{F}_h^{\mathcal{I}}}[\![v]\!]_N \cdot \{\!\!\{\overline{\nabla_h v}\}\!\!\}\,\mathrm{d}S\right) - 2\,\mathrm{Re}\,\left(\int_{\mathcal{F}_h^{\mathcal{B}}}\delta\,v\,\overline{\nabla_h v \cdot \boldsymbol{n}}\,\mathrm{d}S\right) \\
&\quad + \mathrm{i}\omega^{-1}\|\beta^{1/2}[\![\nabla_h v]\!]_N\|_{0,\mathcal{F}_h^{\mathcal{I}}}^2 + \mathrm{i}\omega^{-1}\|\delta^{1/2}\nabla_h v \cdot \boldsymbol{n}\|_{0,\mathcal{F}_h^{\mathcal{B}}}^2 \\
&\quad + \mathrm{i}\,\|\mathtt{a}^{1/2}\mathtt{h}^{-1/2}[\![v]\!]_N\|_{0,\mathcal{F}_h^{\mathcal{I}}}^2 + \mathrm{i}\omega\,\|(1-\delta)^{1/2}v\|_{0,\mathcal{F}_h^{\mathcal{B}}}^2 + \omega^2\|v\|_{0,\Omega}^2. \tag{4.5}
\end{aligned}$$

From the weighted Cauchy-Schwarz inequality and the Young inequality, we obtain, for $s > 0$ at disposal,

$$\begin{aligned}
\left|2\,\mathrm{Re}\,\int_{\mathcal{F}_h^{\mathcal{I}}}[\![v]\!]_N \cdot \{\!\!\{\overline{\nabla_h v}\}\!\!\}\,\mathrm{d}S\right| &\leq s\,\|\mathtt{h}^{-1/2}[\![v]\!]_N\|_{0,\mathcal{F}_h^{\mathcal{I}}}^2 + \frac{1}{s}\,\|\mathtt{h}^{1/2}\{\!\!\{\nabla_h v\}\!\!\}\|_{0,\mathcal{F}_h^{\mathcal{I}}}^2 \\
&\leq \frac{s}{\mathtt{a}_{\min}}\,\|\mathtt{a}^{1/2}\mathtt{h}^{-1/2}[\![v]\!]_N\|_{0,\mathcal{F}_h^{\mathcal{I}}}^2 + \frac{C_{\mathrm{tinv}}^2}{s}\,\|\nabla_h v\|_{0,\Omega}^2, \tag{4.6}
\end{aligned}$$

where in the last step we have used the inverse inequality of Theorem 3.7; similarly, for $t > 0$ at disposal, we have

$$\left|2\,\mathrm{Re}\,\int_{\mathcal{F}_h^{\mathcal{B}}}\delta\,v\,\overline{\nabla_h v}\,\mathrm{d}S\right| \leq t\,\omega\,\frac{\delta}{1-\delta}\,\|(1-\delta)^{1/2}v\|_{0,\mathcal{F}_h^{\mathcal{B}}}^2 + \frac{1}{t\,\omega}\,\|\delta^{1/2}\nabla_h v\|_{0,\mathcal{F}_h^{\mathcal{B}}}^2. \tag{4.7}$$

Since $0 < \delta < 1/2$ and $\mathtt{a}_{\min} > C_{\text{tinv}}^2$, if s and t are such that $s > C_{\text{inv}}^2$ and $t > 1$, inserting (4.6) and (4.5) into (4.5) gives

$$
\begin{aligned}
|b_h(v,v)| &\geq \frac{1}{\sqrt{2}} \left[|\text{Re}\ (b_h(v,v))| + |\text{Im}\ (b_h(v,v))| \right] \\
&\geq \frac{1}{\sqrt{2}} \Bigg[\left(1 - \frac{C_{\text{tinv}}^2}{s} \right) \|\nabla_h v\|_{0,\Omega}^2 + \left(1 - \frac{s}{\mathtt{a}_{\min}} \right) \|\mathtt{a}^{1/2}\mathtt{h}^{-1/2} [\![v]\!]_N\|_{0,\mathcal{F}_h^{\mathcal{I}}}^2 \\
&\quad + \omega \left(1 - t\frac{\delta}{1-\delta} \right) \|(1-\delta)^{1/2}v\|_{0,\mathcal{F}_h^{\mathcal{B}}}^2 + \omega^{-1}\left(1 - \frac{1}{t} \right) \|\delta^{1/2}\nabla_h v \cdot \boldsymbol{n}\|_{0,\mathcal{F}_h^{\mathcal{B}}}^2 \\
&\quad + \omega^{-1}\|\beta^{1/2}[\![\nabla_h v]\!]_N\|_{0,\mathcal{F}_h^{\mathcal{I}}}^2 + \omega^2\|v\|_{0,\Omega}^2 \Bigg] \geq C\|v\|_{DG}^2,
\end{aligned}
$$

with $C > 0$ independent of the mesh and ω. $\qquad \square$

Remark 4.3. For the original formulation of Cessenat and Després [10] where $\mathtt{a} = \omega\mathtt{h}/2$, the coercivity stated in Proposition 4.2 remains elusive. Still, Proposition 4.1 confirms existence and uniqueness of discrete solutions, which Cessenat and Després proved in a completely different fashion.

We develop the theoretical analysis of the method (4.2) by using Schatz' duality argument [30]. We start by stating the following abstract estimate.

Proposition 4.4. *If u is the analytical solution to* (1.1) *and $u_h \in V_h$ defined as in* (4.1) *is the discrete solution to* (2.7) *with numerical fluxes* (2.8) *and* (2.9) *(α and δ as in Prop. 4.2), then*

$$
\|u - u_h\|_{DG} \leq C_{\text{abs}} \left(\inf_{v_h \in V_h} \|u - v_h\|_{DG+} + \sup_{0 \neq w_h \in V_h} \frac{\omega\,|(u - u_h, w_h)|}{\|w_h\|_{0,\Omega}} \right), \tag{4.8}
$$

where $C_{\text{abs}} = C_{\text{abs}}(\Omega, \alpha_0, p) > 0$ is a constant independent of the mesh and ω.

Proof. By the triangle inequality, for all $v_h \in V_h$, it holds

$$
\|u - u_h\|_{DG} \leq \|u - v_h\|_{DG} + \|v_h - u_h\|_{DG}. \tag{4.9}
$$

From the coercivity in Proposition 4.2, the definition of $b_h(\cdot, \cdot)$ and (4.4), we get

$$
\begin{aligned}
\|v_h - u_h\|_{DG}^2 &\leq \frac{1}{C_{\text{coer}}} |b_h(v_h - u_h, v_h - u_h)| \\
&\leq \frac{1}{C_{\text{coer}}} |b_h(v_h - u, v_h - u_h)| + \frac{1}{C_{\text{coer}}} |b_h(u - u_h, v_h - u_h)| \\
&= \frac{1}{C_{\text{coer}}} |b_h(v_h - u, v_h - u_h)| + \frac{1}{C_{\text{coer}}} 2\omega^2|(u - u_h, v_h - u_h)|. \tag{4.10}
\end{aligned}
$$

We estimate the first term on the right-hand side of (4.10). Setting $w_h := v_h - u_h$, integrating by parts and taking into account that $-\Delta w_h = \omega^2 w_h$ in each $K \in \mathcal{T}_h$, we can write

$$
\begin{aligned}
(\nabla_h(v_h - u), \nabla_h w_h) &= \sum_{K \in \mathcal{T}_h} \left[-\int_K (v_h - u)\overline{\Delta w_h}\, dV + \int_{\partial K} (v_h - u)\overline{\nabla_h w_h \cdot \boldsymbol{n}}\, dS \right] \\
&= \omega^2(v_h - u, w_h) + \int_{\mathcal{F}_h^{\mathcal{I}}} [\![v_h - u]\!]_N \cdot \{\!\!\{\overline{\nabla_h w_h}\}\!\!\}\, dS \\
&\quad + \int_{\mathcal{F}_h^{\mathcal{I}}} \{\!\!\{v_h - u\}\!\!\}[\![\overline{\nabla_h w_h}]\!]_N\, dS + \int_{\mathcal{F}_h^{\mathcal{B}}} (v_h - u)\overline{\nabla_h w_h \cdot \boldsymbol{n}}\, dS,
\end{aligned}
$$

where we have used the usual "DG magic formula" to write the sum over all elements of integrals over element boundaries as in terms of integrals over the mesh skeleton. Thus, using the definition of $b_h(\cdot,\cdot)$, we have

$$
\begin{aligned}
b_h(v_h - u, w_h) = {} & 2\,\omega^2(v_h - u, w_h) + \int_{\mathcal{F}_h^{\mathcal{I}}} \{\!\{v_h - u\}\!\} [\![\overline{\nabla_h w_h}]\!]_N \, \mathrm{d}S \\
& + \int_{\mathcal{F}_h^{\mathcal{B}}} (v_h - u)\overline{\nabla_h w_h \cdot \boldsymbol{n}} \, \mathrm{d}S - \int_{\mathcal{F}_h^{\mathcal{I}}} \{\!\{\nabla_h(v_h - u)\}\!\} \cdot [\![w_h]\!]_N \, \mathrm{d}S \\
& - \int_{\mathcal{F}_h^{\mathcal{B}}} \delta(v_h - u)\overline{\nabla_h w_h \cdot \boldsymbol{n}} \, \mathrm{d}S - \int_{\mathcal{F}_h^{\mathcal{B}}} \delta \nabla_h(v_h - u) \cdot \boldsymbol{n}\, \overline{w_h} \, \mathrm{d}S \\
& + \frac{\mathrm{i}}{\omega} \int_{\mathcal{F}_h^{\mathcal{I}}} \beta [\![\nabla_h(v_h - u)]\!]_N [\![\overline{\nabla_h w_h}]\!]_N \, \mathrm{d}S \\
& + \frac{\mathrm{i}}{\omega} \int_{\mathcal{F}_h^{\mathcal{B}}} \delta \nabla_h(v_h - u) \cdot \boldsymbol{n}\, \overline{\nabla_h w_h \cdot \boldsymbol{n}} \, \mathrm{d}S \\
& + \mathrm{i} \int_{\mathcal{F}_h^{\mathcal{I}}} \frac{\mathsf{a}}{\mathsf{h}} [\![v_h - u]\!]_N [\![\overline{w_h}]\!] \, \mathrm{d}S + \mathrm{i}\omega \int_{\mathcal{F}_h^{\mathcal{B}}} (1 - \delta)(v_h - u)\overline{w_h} \, \mathrm{d}S.
\end{aligned}
$$

Therefore, by repeatedly applying the Cauchy-Schwarz inequality with appropriate weights, we obtain

$$
|b_h(v_h - u, w_h)| \leq C\, \|v_h - u\|_{DG^+} \|w_h\|_{DG},
$$

with $C > 0$ only depending on α_0 and p. Inserting this into (4.10) and taking into account (4.9) gives the result. $\qquad\square$

We have to bound the term $\displaystyle\sup_{0 \neq w_h \in V_h} \frac{\omega\,|(u - u_h, w_h)|}{\|w_h\|_{0,\Omega}}$ in the estimate of Proposition 4.4 by using a duality argument. To this end, we have to adopt the special choice (2.13) of all the numerical flux parameters, with the additional constraints $\mathsf{a}_{\min} > C_{\mathrm{tinv}}^2$ and $0 < \delta < 1/2$. Then the DG seminorm and norms can be explicitly written as follows:

$$
\begin{aligned}
|v|_{DG}^2 = {} & \|\nabla_h v\|_{0,\Omega}^2 + \|\mathsf{b}^{1/2}\mathsf{h}^{1/2}[\![\nabla_h v]\!]_N\|_{0,\mathcal{F}_h^{\mathcal{I}}}^2 + \|\mathsf{a}^{1/2}\mathsf{h}^{-1/2}[\![v]\!]_N\|_{0,\mathcal{F}_h^{\mathcal{I}}}^2 \\
& + \|\mathsf{d}^{1/2}\mathsf{h}^{1/2}\nabla_h v \cdot \boldsymbol{n}\|_{0,\mathcal{F}_h^{\mathcal{B}}}^2 + \|(\omega - \mathsf{d}\omega^2\mathsf{h})^{1/2}v\|_{0,\mathcal{F}_h^{\mathcal{B}}}^2, \\
\|v\|_{DG}^2 = {} & |v|_{DG}^2 + \omega^2\|v\|_{0,\Omega}^2, \\
\|v\|_{DG^+}^2 = {} & \|v\|_{DG}^2 + \|\mathsf{b}^{-1/2}\mathsf{h}^{-1/2}\{\!\{v\}\!\}\|_{0,\mathcal{F}_h^{\mathcal{I}}}^2 + \|\mathsf{a}^{-1/2}\mathsf{h}^{1/2}\{\!\{\nabla_h v\}\!\}\|_{0,\mathcal{F}_h^{\mathcal{I}}}^2 + \|\mathsf{d}^{-1/2}\mathsf{h}^{-1/2}v\|_{0,\mathcal{F}_h^{\mathcal{B}}}^2.
\end{aligned}
$$

We will make use of the following regularity theorem proved in [26]. Its original statement makes use of the following weighted norm on $H^1(\Omega)$:

$$
\|v\|_{1,\omega,\Omega}^2 = |v|_{1,\Omega}^2 + \omega^2\|v\|_{0,\Omega}^2. \tag{4.11}
$$

Theorem 4.5 ([26], Prop. 8.1.4). *Let Ω be a bounded convex domain (or smooth and star-shaped). Consider the adjoint problem to (1.1) with right-hand side $w \in L^2(\Omega)$:*

$$
\begin{aligned}
-\Delta\varphi - \omega^2\varphi &= w && \text{in } \Omega, \\
-\nabla\varphi \cdot \boldsymbol{n} + \mathrm{i}\omega\,\varphi &= 0 && \text{on } \partial\Omega.
\end{aligned} \tag{4.12}
$$

Then, the solution φ belongs to $H^2(\Omega)$, and

$$\|\varphi\|_{1,\omega,\Omega} \leq C_1 \text{diam}(\Omega)\|w\|_{0,\Omega},$$
$$|\varphi|_{2,\Omega} \leq C_2 \left(1 + \text{diam}(\Omega)\omega\right)\|w\|_{0,\Omega}, \tag{4.13}$$

with $C_1, C_2 > 0$ depending only on the shape of Ω.

The next lemma provides L^2-projection error estimates for traces onto the skeleton of $\mathcal{T}_h$. In light of the definitions of the DG and DG^+ seminorms and norms, these are essential. We keep the notation P_ω for the $L^2(\Omega)$-orthogonal projection onto V_h, see (4.1).

Lemma 4.6. *Let the assumptions of Theorem 4.5 hold true. Then the solution φ of (4.12) allows the estimates*

$$\|\mathsf{h}^{-1/2}(\varphi - \mathsf{P}_\omega\varphi)\|^2_{0,\mathcal{F}_h} \leq C\,h^2(\omega\,h+1)(1+\text{diam}(\Omega)\omega)^2\|w\|^2_{0,\Omega},$$
$$\|\mathsf{h}^{1/2}\nabla_h(\varphi - \mathsf{P}_\omega\varphi)\|^2_{0,\mathcal{F}_h} \leq C\,h^2(\omega\,h+1)^3(1+\text{diam}(\Omega)\omega)^2\|w\|^2_{0,\Omega}, \tag{4.14}$$

with $C = C(\Omega, \alpha_0, p) > 0$ depending only on the bound α_0 for the minimal angle of elements, the number p of plane waves, and the domain Ω.

Proof. We start with local considerations: we recall the multiplicative trace inequality for $K \in \mathcal{T}_h$, see [6], Theorem 1.6.6,

$$\|u\|^2_{0,\partial K} \leq C\|u\|_{0,K}\left(h_K^{-1}\|u\|_{0,K} + |u|_{1,K}\right) \quad \forall u \in H^1(K). \tag{4.15}$$

Here and in the rest of the proof constants $C > 0$ may only depend on the bound for the minimal angle of K, *cf.* Assumption 3.6, p, and the domain Ω. Hence,

$$h_K^{-1}\|\varphi - \mathsf{P}_\omega\varphi\|^2_{0,\partial K} \leq Ch_K^{-1}\|\varphi - \mathsf{P}_\omega\varphi\|_{0,K}\left(h_K^{-1}\|\varphi - \mathsf{P}_\omega\varphi\|_{0,K} + |\varphi - \mathsf{P}_\omega\varphi|_{1,K}\right)$$
$$\leq Ch_K^2(\omega h_K + 1)\left(|\varphi|_{2,K} + \omega^2\|\varphi\|_{0,K}\right)^2,$$

where the last estimate invokes Propositions 3.12 and 3.13. Similarly,

$$h_K\|\nabla_h(\varphi - \mathsf{P}_\omega\varphi)\|^2_{0,\partial K} \leq Ch_K|\varphi - \mathsf{P}_\omega\varphi|_{1,K}\left(h_K^{-1}|\varphi - \mathsf{P}_\omega\varphi|_{1,K} + |\varphi - \mathsf{P}_\omega\varphi|_{2,K}\right)$$
$$\leq Ch_K^2(\omega h_K + 1)^3\left(|\varphi|_{2,K} + \omega^2\|\varphi\|_{0,K}\right)^2.$$

The last step relies on Propositions 3.13 and 3.14. Next, we sum over all elements, apply the Cauchy-Schwarz inequality, and use the estimates (4.13) of Theorem 4.5:

$$\|\mathsf{h}^{-1/2}(\varphi - \mathsf{P}_\omega\varphi)\|^2_{0,\mathcal{F}_h} \leq Ch^2(\omega h+1)(1+\text{diam}(\Omega)\omega)^2\|w\|^2_{0,\Omega},$$
$$\|\mathsf{h}^{1/2}\nabla_h(\varphi - \mathsf{P}_\omega\varphi)\|^2_{0,\mathcal{F}_h} \leq Ch^2(\omega h+1)^3(1+\text{diam}(\Omega)\omega)^2\|w\|^2_{0,\Omega}. \qquad \square$$

Corollary 4.7. *Let the assumptions of Theorem* 4.5 *hold true. Then the solution* φ *of* (4.12) *allows the estimates*

$$\|\varphi - \mathsf{P}_\omega\varphi\|_{0,\Omega}^2 \le Ch^4(1 + \operatorname{diam}(\Omega)\omega)^2\|w\|_{0,\Omega}^2, \tag{4.16}$$

$$\|\varphi - \mathsf{P}_\omega\varphi\|_{DG+}^2 \le Ch^2(\omega\, h + 1)^3(1 + \operatorname{diam}(\Omega)\omega)^2\|w\|_{0,\Omega}^2, \tag{4.17}$$

with $C > 0$ *depending only on the bound for the minimal angle of elements, the number p of plane waves, the geometry of* Ω, *and the parameters* a, b *and* d *in the definition of the numerical fluxes.*

Proof. The bounds follow from Propositions 3.12, 3.13, Theorem 4.5, Lemma 4.6 and from the bound

$$\|(\omega - \mathtt{d}\omega^2\mathtt{h})^{1/2}v\|_{0,\mathcal{F}_h^\mathcal{B}}^2 \le\ Ch^2(\omega\, h + 1)^3(1 + \operatorname{diam}(\Omega)\omega)^2\|w\|_{0,\Omega}^2,$$

which can be derived with the same arguments as in the proof of Lemma 4.6. $\square$

Proposition 4.8. *Let the assumptions of Theorem* 4.5 *hold true. Then the following estimate holds true:*

$$\sup_{0\ne w_h\in V_h} \frac{\omega|(u - u_h, w_h)|}{\|w_h\|_{0,\Omega}} \le$$
$$C_{\mathrm{dual}} \left[\omega\, h\, (\omega\, h + 1)^{3/2}(1 + \operatorname{diam}(\Omega)\omega)\, \|u - u_h\|_{DG} + \omega\, h^2(1 + \operatorname{diam}(\Omega)\omega)\, \|f - \mathsf{P}_\omega f\|_{0,\Omega} \right],$$

with a constant $C_{\mathrm{dual}} > 0$ *independent of the mesh and* ω, *but dependent on* α_0, *p, the geometry of* Ω *and the parameters* a, b *and* d *in the definition of the numerical fluxes.*

Proof. Consider the adjoint problem (4.12) with right-hand side $w_h \in V_h \subset L^2(\Omega)$. Then, from Theorem 4.5, we have that $\varphi \in H^2(\Omega)$, $\|\varphi\|_{1,\omega,\Omega} \le C_1(\Omega)\|w_h\|_{0,\Omega}$ and $|\varphi|_{2,\Omega} \le C_2(\Omega)\, (1 + \omega)\, \|w_h\|_{0,\Omega}$, with $C_1(\Omega), C_2(\Omega) > 0$. Moreover, this solution φ satisfies

$$a_h(\psi, \varphi) - \omega^2(\psi, \varphi) = (\psi, w_h) \qquad \forall\psi \in V. \tag{4.18}$$

The adjoint consistency of the DG method (see Sect. 2) implies that

$$a_h(\psi_h, \varphi) - \omega^2(\psi_h, \varphi) = (\psi_h, w_h) \qquad \forall\psi_h \in V_h. \tag{4.19}$$

Taking into account adjoint consistency and consistency, *i.e.*, (4.19) and (4.4), respectively, we have, for all $\psi_h \in V_h$,

$$(u - u_h, w_h) = (u, w_h) - (u_h, w_h) \overset{(4.18)}{=} a_h(u, \varphi) - \omega^2(u, \varphi) - (u_h, w_h)$$
$$\overset{(4.19)}{=} a_h(u, \varphi) - \omega^2(u, \varphi) - a_h(u_h, \varphi) + \omega^2(u_h, \varphi)$$
$$= a_h(u - u_h, \varphi) - \omega^2(u - u_h, \varphi)$$
$$\overset{(4.4)}{=} a_h(u - u_h, \varphi - \psi_h) - \omega^2(u - u_h, \varphi - \psi_h).$$

Using the definition of $a_h(\cdot,\cdot)$, integrating by parts the gradient term and taking into account that $-\Delta u - \omega^2 u = f$ and $-\Delta u_h - \omega^2 u_h = 0$ in each $K \in \mathcal{T}_h$, we get

$$
(u - u_h, w_h) = (f, \varphi - \psi_h) + \int_{\mathcal{F}_h^{\mathcal{I}}} [\![\nabla_h(u - u_h)]\!]_N \{\!\!\{\overline{\varphi - \psi_h}\}\!\!\}\, \mathrm{d}S
$$

$$
+ \int_{\mathcal{F}_h^{\mathcal{B}}} \nabla_h(u - u_h) \cdot \boldsymbol{n}\, (\overline{\varphi - \psi_h})\, \mathrm{d}S - \int_{\mathcal{F}_h^{\mathcal{I}}} [\![u - u_h]\!]_N \cdot \{\!\!\{\overline{\nabla_h(\varphi - \psi_h)}\}\!\!\}\, \mathrm{d}S
$$

$$
- \int_{\mathcal{F}_h^{\mathcal{B}}} \mathtt{d}\omega \mathtt{h}\, (u - u_h)\, \overline{\nabla_h(\varphi - \psi_h) \cdot \boldsymbol{n}}\, \mathrm{d}S - \int_{\mathcal{F}_h^{\mathcal{B}}} \mathtt{d}\omega \mathtt{h}\, \nabla_h(u - u_h) \cdot \boldsymbol{n}\, (\overline{\varphi - \psi_h})\, \mathrm{d}S
$$

$$
+ \mathrm{i} \int_{\mathcal{F}_h^{\mathcal{I}}} \mathtt{b}\mathtt{h}\, [\![\nabla_h(u - u_h)]\!]_N \overline{[\![\nabla_h(\varphi - \psi_h)]\!]_N}\, \mathrm{d}S
$$

$$
+ \mathrm{i} \int_{\mathcal{F}_h^{\mathcal{B}}} \mathtt{d}\mathtt{h}\, \nabla_h(u - u_h) \cdot \boldsymbol{n}\, \overline{\nabla_h(\varphi - \psi_h) \cdot \boldsymbol{n}}\, \mathrm{d}S
$$

$$
+ \mathrm{i} \int_{\mathcal{F}_h^{\mathcal{I}}} \frac{\mathtt{a}}{\mathtt{h}}\, [\![u - u_h]\!]_N \cdot \overline{[\![\varphi - \psi_h]\!]_N}\, \mathrm{d}S + \mathrm{i} \int_{\mathcal{F}_h^{\mathcal{B}}} (\omega - \mathtt{d}\omega^2 \mathtt{h})\, (u - u_h)\, (\overline{\varphi - \psi_h})\, \mathrm{d}S
$$

and thus, for all $\psi_h \in V_h$, we obtain

$$
\omega |(u - u_h, w_h)| \leq C\, \|u - u_h\|_{DG}\, \omega \|\varphi - \psi_h\|_{DG^+} + \omega |(f, \varphi - \psi_h)|, \tag{4.20}
$$

with C independent of the mesh, ω, and the flux parameters.

Actually, the estimate (4.20) holds true with $\|\varphi - \psi_h\|_{DG^+}$ replaced by the interelement and boundary part of $\|\varphi - \psi_h\|_{DG^+}$ only (no volume terms).

We choose $\psi_h = \mathsf{P}_\omega \varphi$, *i.e.*, the $L^2(\Omega)$-projection of φ onto V_h. Since

$$
\omega |(f, \varphi - \psi_h)| = \omega |(f - \mathsf{P}_\omega f, \varphi - \psi_h)| \leq \|f - \mathsf{P}_\omega f\|_{0,\Omega}\, \omega \|\varphi - \psi_h\|_{0,\Omega},
$$

the result follows from Corollary 4.7. $\square$

The following estimate of the DG-norm of the error is a direct consequence of Proposition 4.4, Proposition 4.8 and of the following best approximation estimate.

Lemma 4.9. *For any $w \in H^2(\Omega)$, we have*

$$
\inf_{v_h \in V_h} \|w - v_h\|_{DG^+} \leq Ch(\omega h + 1)^{3/2} \left(|w|_{2,\Omega} + \omega^2 \|w\|_{0,\Omega} \right),
$$

with a constant $C = C(\alpha_0, p) > 0$ independent of the mesh and ω.

Proof. We bound $\inf_{v_h \in V_h} \|w - v_h\|_{DG^+}$ by $\|w - \mathsf{P}_\omega w\|_{DG^+}$ and proceed as in Lemma 4.6 and Corollary 4.7. $\square$

Theorem 4.10. *Let the assumptions of Theorem 4.5 hold true and impose $\mathtt{a}_{\min} > C_{\mathrm{tinv}}^2$ and $0 < \delta < \frac{1}{2}$ on the parameters of the plane wave discontinuous Galerkin method (4.2). Then, provided that*

$$
\omega\, h(\omega\, h + 1)^{3/2}(1 + \mathrm{diam}(\Omega)\omega) < \frac{1}{C_{\mathrm{abs}} C_{\mathrm{dual}}}, \tag{4.21}
$$

the following a priori *error estimate holds true:*

$$
\|u - u_h\|_{DG} \leq Ch \left[|u|_{2,\Omega} + \omega^2 \|u\|_{0,\Omega} + \|f - \mathsf{P}_\omega f\|_{0,\Omega} \right],
$$

with a constant $C = C(\Omega, \alpha_0, p) > 0$ independent of the mesh and wave number ω.

Proof. From Propositions 4.4 and 4.8, provided that (4.21) is satisfied, we have

$$\|u - u_h\|_{DG} \leq C \left[\inf_{v_h \in V_h} \|u - v_h\|_{DG^+} + \omega\, h^2 (1 + \mathrm{diam}(\Omega)\omega)\, \|f - \mathsf{P}_\omega f\|_{0,\Omega} \right],$$

with a constant $C > 0$ independent of the mesh and ω. The result now follows from the regularity of u, Lemma 4.9 and the fact that (4.21) implies that both $\omega\, h$ and $\omega^2 h\, \mathrm{diam}(\Omega)$ are bounded by $1/C_{\mathrm{abs}}C_{\mathrm{dual}}$. $\square$

Remark 4.11. The threshold condition (4.21) imposes a minimum resolution of the trial space before asymptotic convergence sets in. In the relevant case of $\omega > 1$, this is equivalent to demanding that $\omega^2 h$ be sufficiently small. This reflects vulnerability to the *pollution effect* discussed in the Introduction, which is confirmed by numerical experiments in Section 5. As a consequence, the h-version of the plane wave discontinuous Galerkin methods will require prohibitively fine meshes, if Ω accommodates many wavelengths.

Remark 4.12. The mere first-order convergence asserted in Theorem 4.10 may be disappointing, but in the presence of a non-vanishing source term f no better rate can be expected, because plane waves only possess the approximating power of 1st-degree polynomials for generic functions, see Section 3.2.

Only solution of the homogeneous Helmholtz equation, that is, the case $f = 0$, allows better approximation estimates when using more plane wave directions. More precisely, if u is sufficiently smooth and $p = 2m+1$, we can expect $\|u - u_h\|_{DG} = O(h^m)$. The underlying approximation results are given in [26], Proposition 8.4.14. In this paper we will not elaborate this further in the DG setting.

We conclude this section by proving *a priori* L^2-norm error estimates. We have the following result:

Theorem 4.13. *Let the assumptions of Theorem 4.5 hold true. Then, provided that the threshold condition (4.21) is satisfied, we have*

$$\|u - u_h\|_{0,\Omega} \leq Ch^2(1 + \mathrm{diam}(\Omega)\omega) \left[|u|_{2,\Omega} + \omega^2 \|u\|_{0,\Omega} + \|f - \mathsf{P}_\omega f\|_{0,\Omega} \right),$$

with a constant $C > 0$ independent of the mesh and wave number ω, but dependent on α_0, p, the geometry of Ω and the parameters $\mathtt{a}$, $\mathtt{b}$ *and* $\mathtt{d}$ *in the definition of the numerical fluxes.*

Proof. Let φ be the solution to the adjoint problem (4.12) with right-hand side $w \in L^2(\Omega)$. By proceeding like in the proof of Proposition 4.8, by definition of the dual problem, consistency and adjoint consistency, we have

$$(u - u_h, w) = a_h(u - u_h, \varphi - \mathsf{P}_\omega\varphi) - \omega^2(u - u_h, \varphi - \mathsf{P}_\omega\varphi),$$

or, equivalently,

$$\begin{aligned} (u - u_h, w) = {} & a_h(u - v_h, \varphi - \mathsf{P}_\omega\varphi) - \omega^2(u - v_h, \varphi - \mathsf{P}_\omega\varphi) \\ & + a_h(v_h - u_h, \varphi - \mathsf{P}_\omega\varphi) - \omega^2(v_h - u_h, \varphi - \mathsf{P}_\omega\varphi) \end{aligned} \qquad (4.22)$$

for all $v_h \in V_h$. By repeatedly applying the Cauchy-Schwarz inequality with appropriate weights, we obtain

$$|a_h(u - v_h, \varphi - \mathsf{P}_\omega\varphi) - \omega^2(u - v_h, \varphi - \mathsf{P}_\omega\varphi)| \leq \|u - v_h\|_{DG^+}\|\varphi - \mathsf{P}_\omega\varphi\|_{DG^+},$$

whereas, since $v_h - u_h \in V_h$, proceeding as in the proof of Proposition 4.4, we get

$$|a_h(v_h - u_h, \varphi - \mathsf{P}_\omega\varphi) - \omega^2(v_h - u_h, \varphi - \mathsf{P}_\omega\varphi)| \leq \|v_h - u_h\|_{DG}\|\varphi - \mathsf{P}_\omega\varphi\|_{DG^+}.$$

By applying these estimates to the right-hand side of (4.22), we obtain

$$\begin{aligned} |(u - u_h, w)| & \leq (\|u - v_h\|_{DG^+} + \|v_h - u_h\|_{DG})\, \|\varphi - \mathsf{P}_\omega\varphi\|_{DG^+} \\ & \leq (2\|u - v_h\|_{DG^+} + \|u - u_h\|_{DG})\, \|\varphi - \mathsf{P}_\omega\varphi\|_{DG^+} \end{aligned}$$

for all $v_h \in V_h$. From the definition of the L^2-norm we have

$$\|u - u_h\|_{0,\Omega} \leq \left(2 \inf_{v_h \in V_h} \|u - v_h\|_{DG^+} + \|u - u_h\|_{DG} \right) \sup_{0 \neq w \in L^2(\Omega)} \frac{\|\varphi - \mathsf{P}_\omega \varphi\|_{DG^+}}{\|w\|_{0,\Omega}}.$$

The result follows from Lemma 4.9, Theorem 4.10 and Corollary 4.7. $\qquad\square$

Remark 4.14. Theorem 4.13 states quadratic convergence of the L^2-norm of the error, under the threshold condition (4.21); on the other hand, the constant in the error estimate deteriorates linearly with increasing wavenumbers.

Remark 4.15. In [7], an *a priori* L^2-norm error estimate of the form

$$\|u - u_h\|_{0,\Omega} \leq C h^{-1/2} \inf_{v_h \in X_h} \|u - v_h\|_X \tag{4.23}$$

for h-version of the UWVF is directly established. It is valid for $f = 0$ and relies on an error estimate in a mesh-dependent norm proved in [10]. Here, $\|\cdot\|_X$ is a scaled L^2-norm on the skeleton of the mesh and X_h a plane wave type space. In contrast to our results, this estimate holds for all wave numbers, but the dependence of C on ω is not made explicit.

For sufficiently smooth analytical solutions (4.23) yields $O(h^{m-1})$-convergence when using $p = 2m + 1$ equispaced plane wave directions. The authors point out that numerical tests show that this under-estimates the actual convergence rates and conjecture that this gap might be filled by using duality arguments. It might be of interest to investigate whether our approach could actually be useful in this direction (see Rem. 4.12).

5. NUMERICAL EXPERIMENTS

In a series of numerical experiments in 2D we study the convergence of the h-version of different primal plane wave discontinuous Galerkin methods. We consider (1.1) on simple bounded domains $\Omega \subset \mathbb{R}^2$ and fix source terms f and g such that u agrees with a prescribed analytic solution. All the computations were done in MATLAB on fairly uniform unstructured triangular meshes.

Experiment 1 studies the *homogeneous* Helmholtz boundary value problem (1.1) ($f = 0$) on the unit square $\Omega :=]0,1[^2$. We impose an outgoing cylindrical wave solution

$$u(\boldsymbol{x}) = H_0^{(1)}(\omega|\boldsymbol{x} - \boldsymbol{x}_0|), \quad \boldsymbol{x}_0 = \begin{pmatrix} -1/4 \\ 0 \end{pmatrix}, \tag{5.1}$$

where $H_0^{(1)}$ is the zero-th order Hankel function of the first kind.

The experiment seeks to explore

(1) the relative performance of different versions of the mixed discontinuous Galerkin approach (2.7), which differ in the choice of the parameters α, β, and γ in the numerical fluxes (2.8), (2.9), see Table 1;

(2) the presence and strength of the pollution effect, by monitoring the onset of asymptotic convergence and its dependence on ωh as well as the increase of the discretization error for increasing ω and fixed ωh.

A sequence of unstructured triangular meshes of different resolution (measured in terms of the maximal edge length h) was used. It was produced by a mesh generator. Figure 6 gives an impression of what these meshes look like. We measure the discretization error in the broken version of the weighted norm ("energy norm") (4.11)

$$\|v\|_{1,\omega,h}^2 := \|\nabla_h v\|_{0,\Omega}^2 + \omega^2 \|v\|_{0,\Omega}^2, \tag{5.2}$$

and in the $L^2(\Omega)$-norm.

TABLE 1. Choice of parameters for numerical fluxes (2.8), (2.9), (2.14), with different plane wave DG methods. Here, C denotes an estimate for C_{tinv} from Theorem 3.7. We computed C_{tinv} on each element using (3.30) in the plane wave basis and defined C on each edge as the maximal value of C_{tinv} on the neighboring elements.

Method	α	β	γ	δ	λ
UWVF [10]	$\frac{1}{2}$	$\frac{1}{2}$	0	$\frac{1}{2}$	$\frac{1}{2}$
PWDG0	$\frac{2}{\omega h}$	0	0	0	$\frac{2}{\omega h}$
PWDG1	$\frac{C^2}{2\omega h}$	0	0	0	$\frac{C^2}{\omega h}$
PWDG2	$\frac{C^2}{2\omega h}$	$\frac{\omega h}{10}$	0	$\min\{\frac{1}{2}, \frac{\omega h}{10}\}$	$\frac{C^2}{\omega h}$

2D triangular mesh

\# Vertices : 13,   \# Elements : 14,   \# Edges : 26

2D triangular mesh

\# Vertices : 32,   \# Elements : 44,   \# Edges : 75
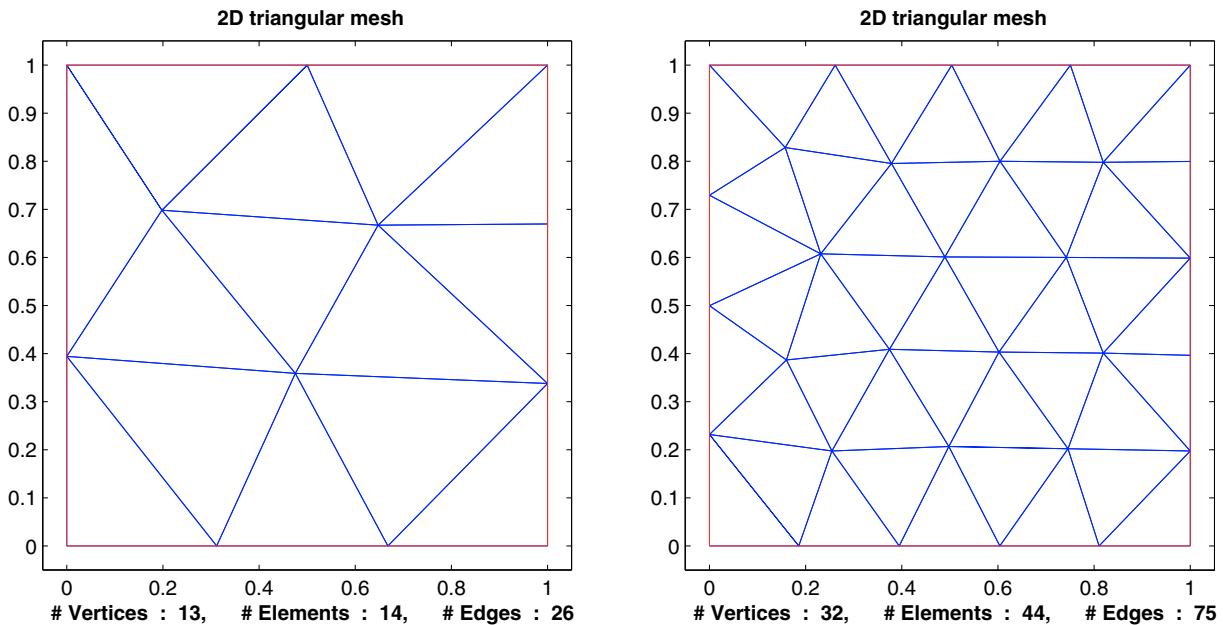
FIGURE 6. The third and fifth coarsest meshes on the unit square.

We observe algebraic convergence in terms of $h\omega$ for all methods and $p = 5$, see Figures 7 and 8. All the methods offer about the same accuracy and convergence rates. The plots hint at a slightly worse convergence for the classical UWVF, which does not comply with the assumptions of the theory of Section 4.

In Figure 9 we notice faster algebraic convergence when using more plane wave directions in the local trial spaces, *cf.* Remark 4.12.

Figures 8 and 10 highlight delayed onset of algebraic convergence for high wavenumbers. Moreover, the plane wave DG solutions fails to come close to the best approximation of the exact solution in the trial space. Thus, keeping ωh small, which guarantees uniformly accurate best approximation in plane wave space, fails to control the Galerkin discretization error for increasing ω, see Figure 11. All this is clear evidence that the pollution effect also affects plane wave DG methods, *cf.* Remark 4.11.
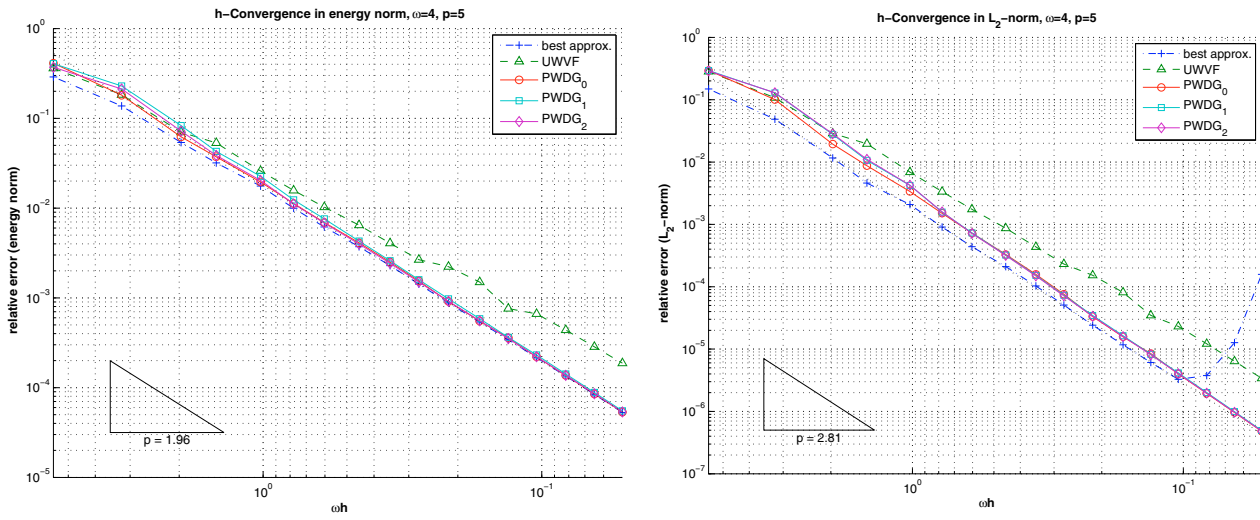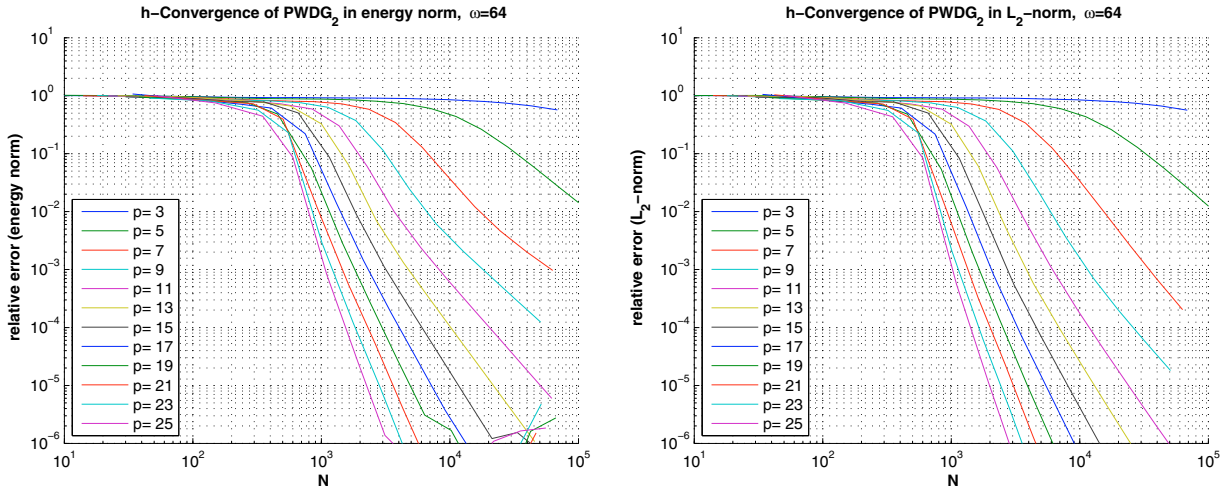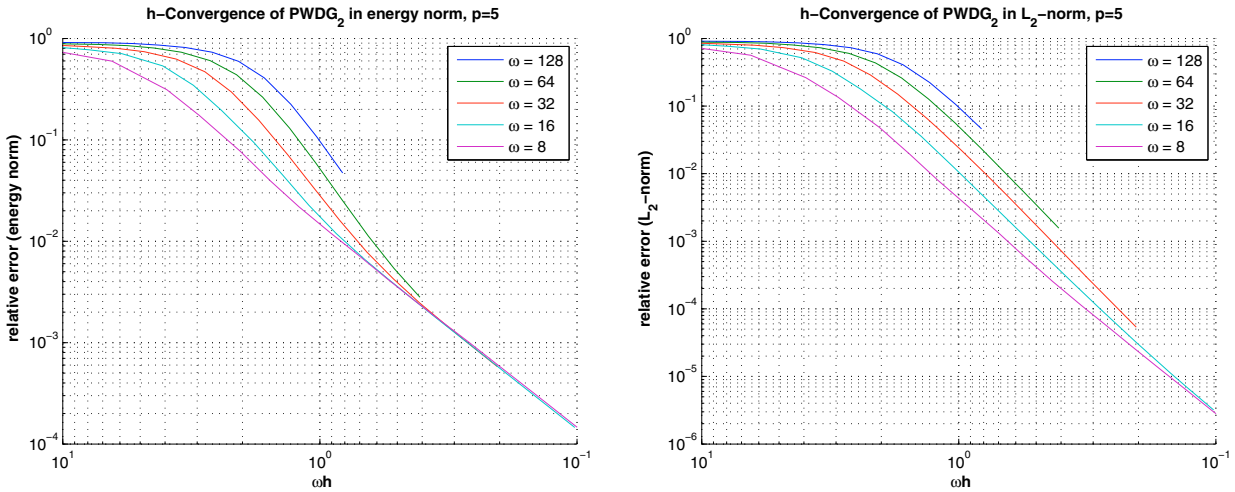
FIGURE 7. Experiment 1: *h*-convergence of PWDG methods for $\omega = 4$. The relative errors in the energy norm (5.2) and the L^2-norm are plotted against ωh. The divergence of the best approximation in the L^2-norm is due to numerical instability in the computation of the L^2-projection using the exponential basis.
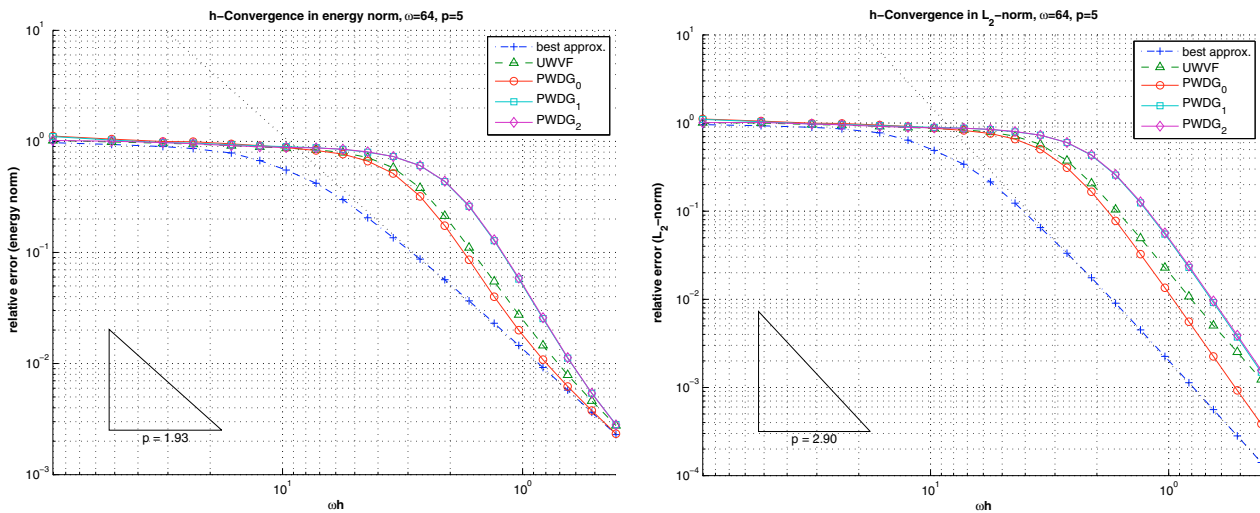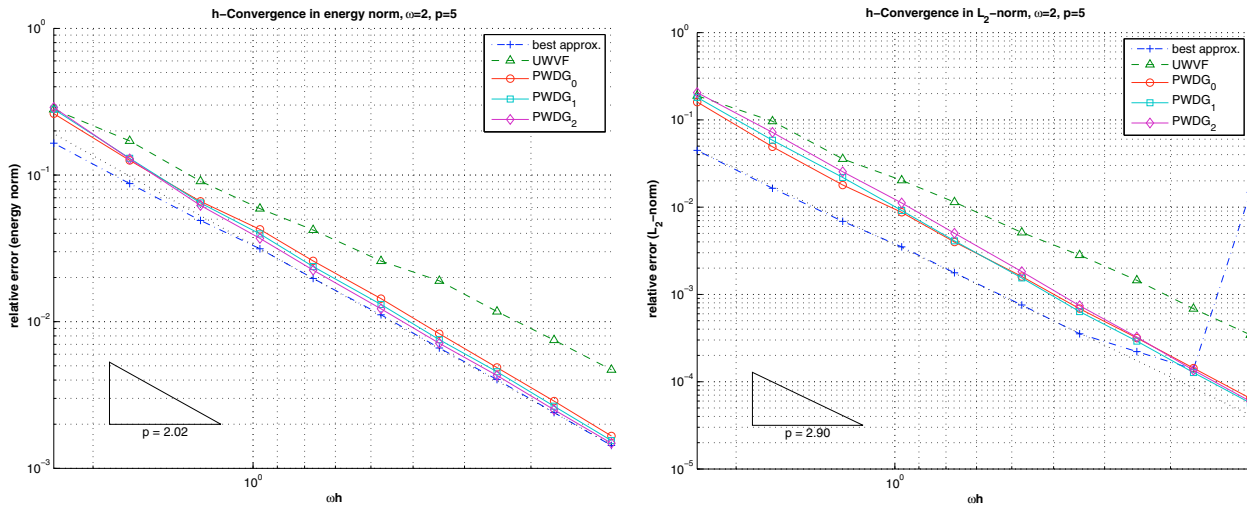

FIGURE 8. Experiment 1: *h*-convergence of PWDG methods for $\omega = 64$. The relative errors in the energy norm (5.2) and the L^2-norm are plotted against ωh.

Experiment 2 conducts similar investigations as Experiment 1 for the realistic setting of plane wave scattering at a sound soft circular object (Fig. 12). Spatial discretization is carried out in an annulus $\Omega := \{\boldsymbol{x} \in \mathbb{R}^2 : 1 < |\boldsymbol{x}| < 3\}$ and the exterior inhomogeneous impedance boundary conditions allow for the exact Mie solution

FIGURE 9. Experiment 1: h-convergence of PWDG2 for various values of p. The relative errors in the energy norm (5.2) and the L^2-norm are plotted against the number N of degrees of freedom.
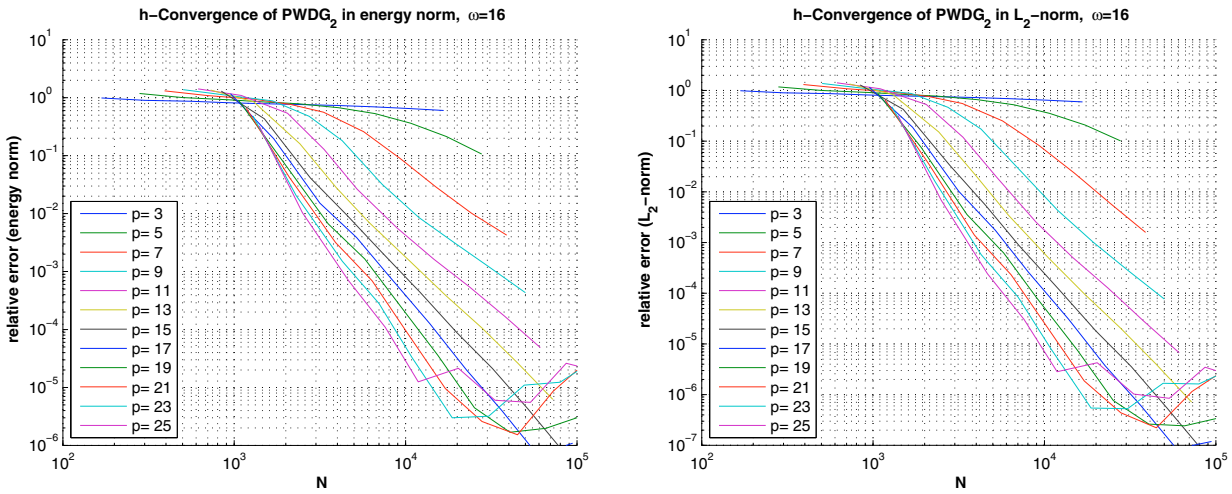

FIGURE 10. Experiment 1: h-convergence of PWDG2 for various values of ω. The relative errors in the energy norm (5.2) and the L^2-norm are plotted against ωh.

to the problem,

$$u(r, \varphi) = -\frac{J_0(\omega)}{H_0^{(2)}(\omega)} H_0^{(2)}(\omega r) - 2 \sum_{n=1}^{\infty} \mathrm{i}^n \frac{J_n(\omega)}{H_n^{(2)}(\omega)} H_n^{(2)}(\omega r) \cos(n\varphi). \tag{5.3}$$

Dirichlet boundary conditions corresponding to the negative of the incoming wave $\exp(\mathrm{i}\omega \binom{1}{0} \cdot \boldsymbol{x})$ are imposed on the inner circle.
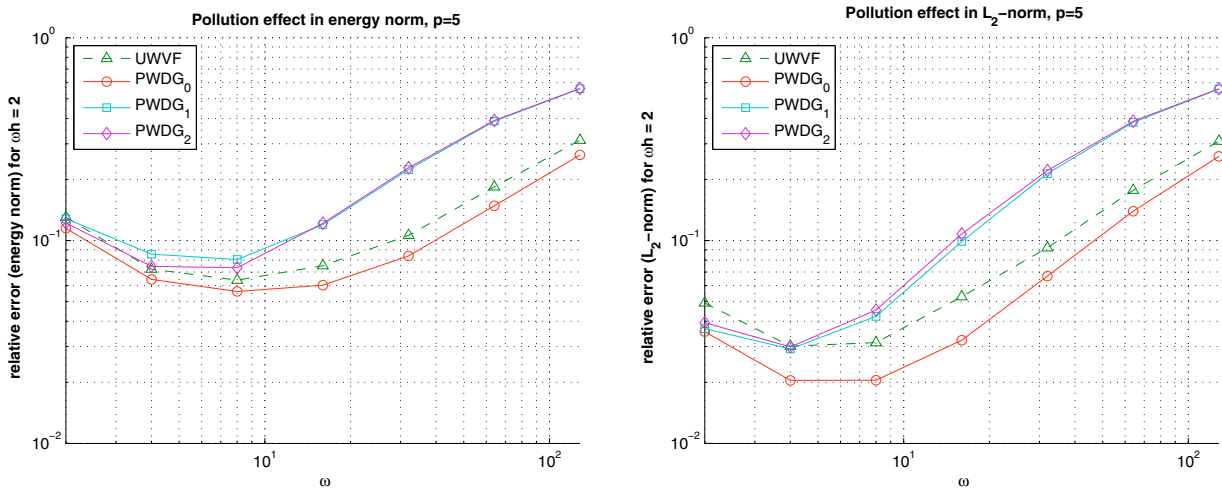
FIGURE 11. Experiment 1: errors of PWDG methods for fixed $\omega h = 2$ and variable ω. Values were computed by linear interpolation (w.r.t. h) of data points in bilogarithmic scale.
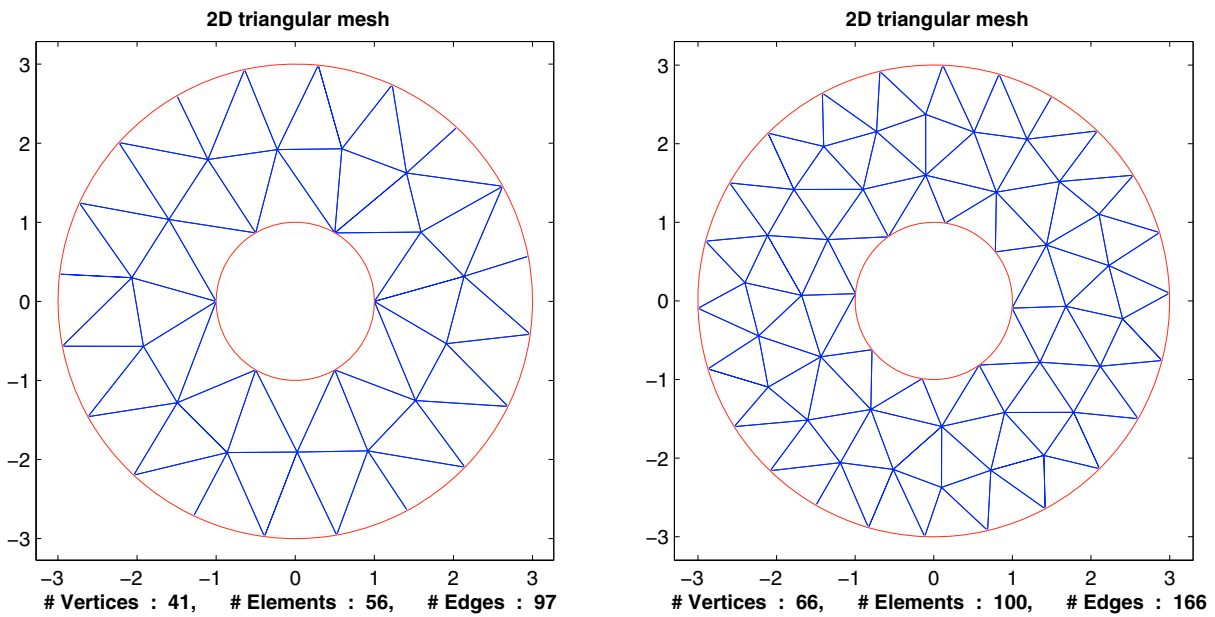
FIGURE 12. Experiment 2: the two coarsest meshes on the annulus.

The circular boundary is exactly taken into account by using an analytic parameterization. The evaluation of the matrix entries relies on high order Gaussian quadrature rules which produce negligible quadrature error for all wave numbers ω used in this experiment.
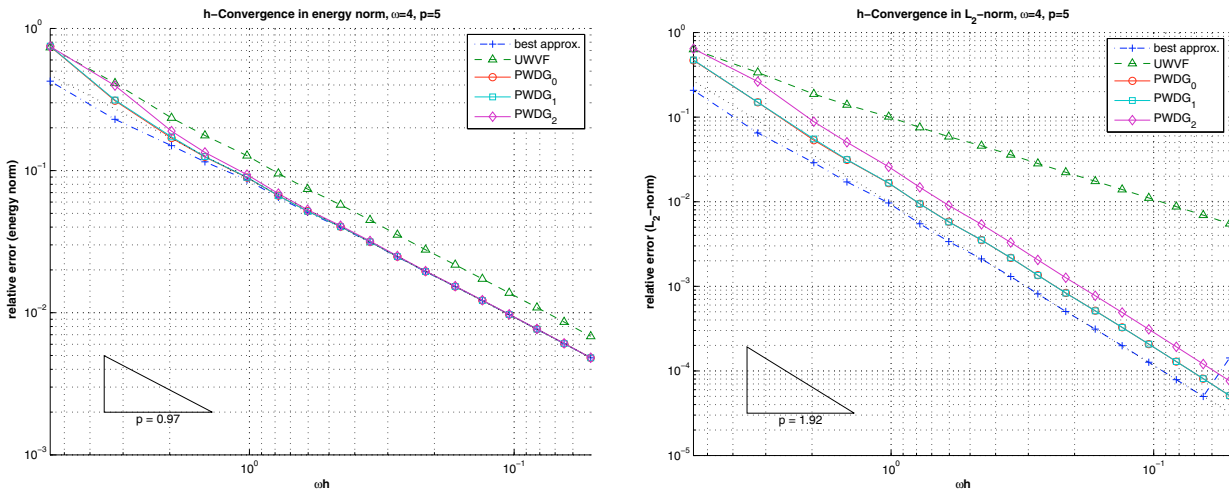
FIGURE 13. Experiment 2: h-convergence of PWDG methods for $\omega = 2$. The relative errors in the energy norm (5.2) and the L^2-norm are plotted against ωh.
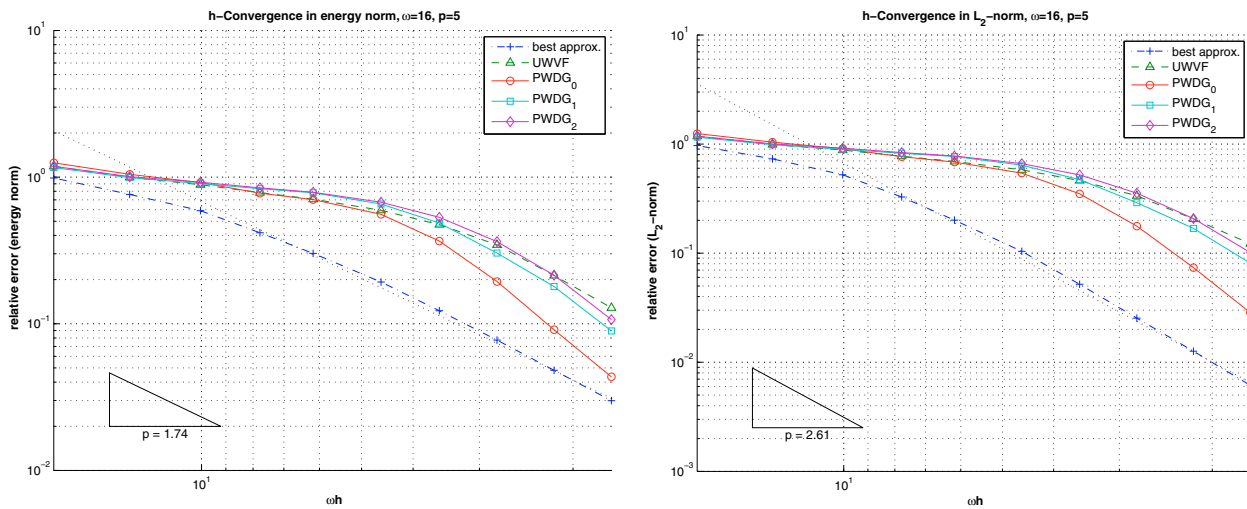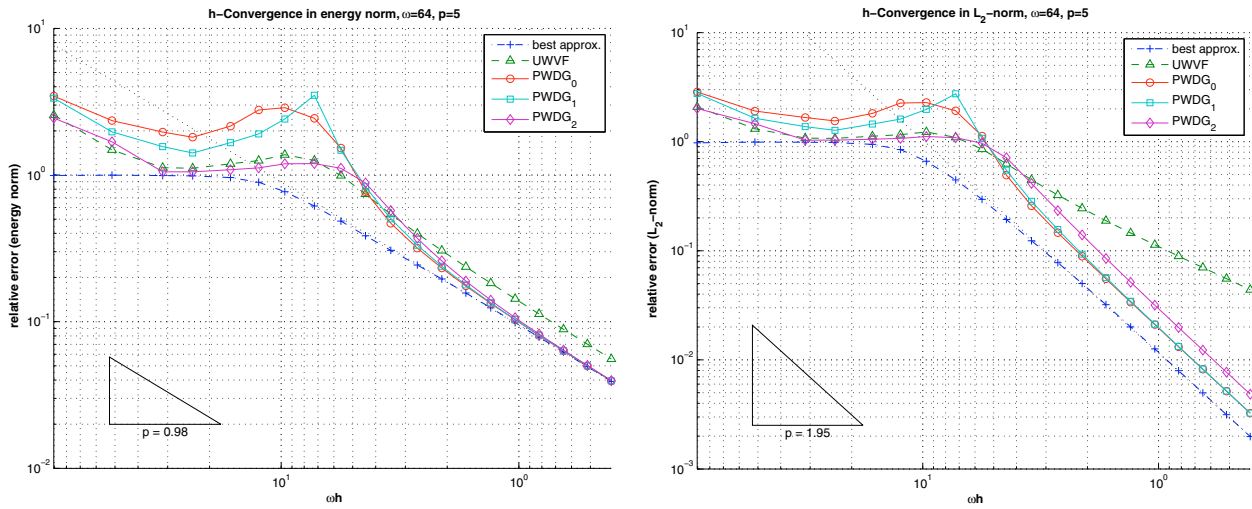

FIGURE 14. Experiment 2: h-convergence of PWDG2 for $\omega = 16$. The relative errors in the energy norm (5.2) and the L^2-norm are plotted against ωh.

By and large, in Experiment 2 we make the same observations as in Experiment 1, see Figures 13 through 15.

Experiment 3 studies the *inhomogeneous* Helmholtz boundary value problem (1.1), *i.e.*, $f \neq 0$. As solution we impose a circular wave (5.1) belonging to the "wrong" frequency $\frac{1}{2}\omega$. Again, $\Omega :=]0, 1[^2$.

FIGURE 15. Experiment 2: h-convergence of PWDG2 for various values of p. The relative errors in the energy norm (5.2) and the L^2-norm are plotted against the number N of degrees of freedom.

FIGURE 16. Experiment 3: h-convergence of PWDG methods for $\omega = 4$. The relative errors in the energy norm (5.2) and the L^2-norm are plotted against ωh.

Again, for $p = 5$, we observe algebraic convergence in ωh in all norms examined, see Figures 16 and 17. The classical UWVF suffers reduced order of convergence in $L^2(\Omega)$-norm. Figure 18 demonstrates that for this inhomogeneous Helmholtz problem raising p does not give better accuracy, *cf.* Remark 4.12.

FIGURE 17. Experiment 3: *h*-convergence of PWDG methods for $\omega = 64$. The relative errors in the energy norm (5.2) and the L^2-norm are plotted against ωh.
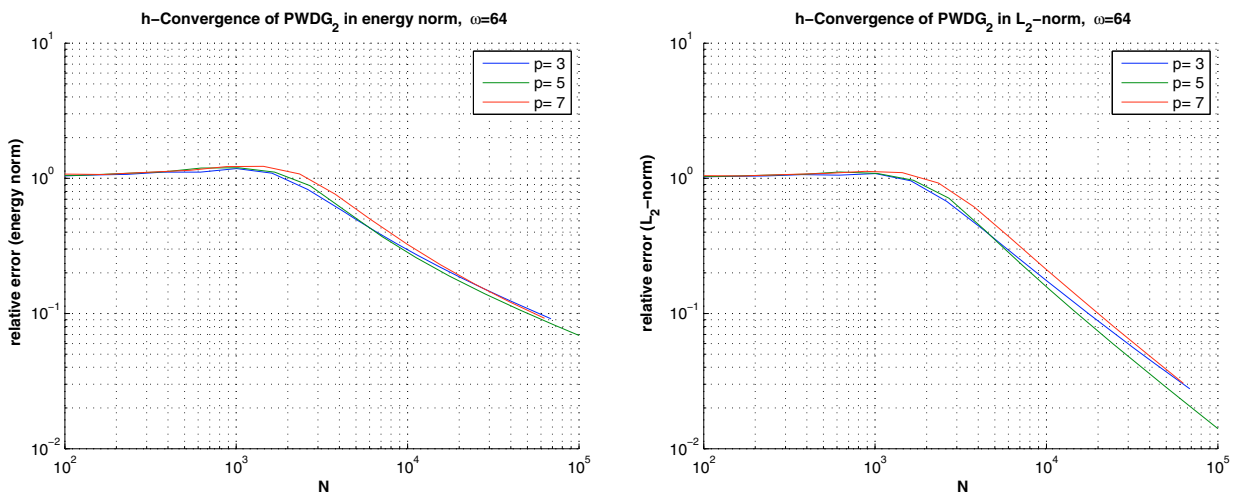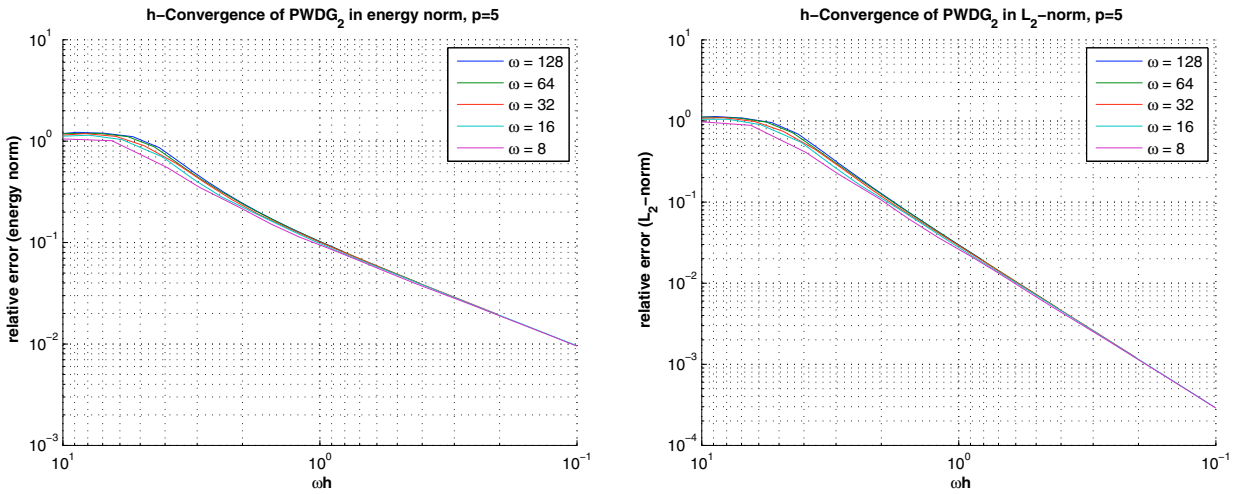

FIGURE 18. Experiment 3: *h*-convergence of PWDG2 for various values of *p*. The relative errors in the energy norm (5.2) and the L^2-norm are plotted against the number *N* of degrees of freedom.

Figures 19 and 20 hint at a significantly reduced pollution effect in this experiment, for which the solution is not a propagating wave.

FIGURE 19. Experiment 3: h-convergence of PWDG2 for various values of ω. The relative errors in the energy norm (5.2) and the L^2-norm are plotted against ωh.
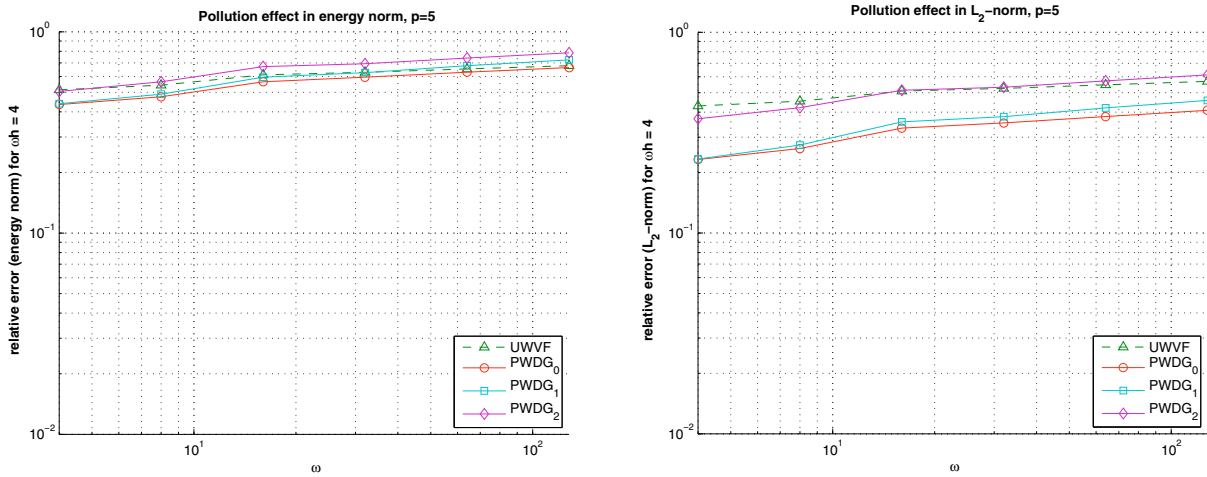

FIGURE 20. Experiment 3: errors of PWDG methods for fixed $\omega h = 4$ and variable ω, *cf.* Figure 11.

REFERENCES

[1] M. Ainsworth, Discrete dispersion relation for hp-version finite element approximation at high wave number. *SIAM J. Numer. Anal.* **42** (2004) 563–575.

[2] D. Arnold, F. Brezzi, B. Cockburn and L. Marini, Unified analysis of discontinuous Galerkin methods for elliptic problems. *SIAM J. Numer. Anal.* **39** (2002) 1749–1779.

[3] I. Babuška and J. Melenk, The partition of unity method. *Int. J. Numer. Methods Eng.* **40** (1997) 727–758.

[4] I. Babuška and S. Sauter, Is the pollution effect of the FEM avoidable for the Helmholtz equation? *SIAM Review* **42** (2000) 451–484.

[5] L. Banjai and S. Sauter, *A refined Galerkin error and stability analysis for highly indefinite variational problems.* Report 03-06, Institut für Mathematik, Universität Zürich, Zürich, Switzerland (2006).

[6] S. Brenner and R. Scott, *Mathematical theory of finite element methods, Texts in Applied Mathematics.* Springer-Verlag, New York, 2nd edn. (2002).

[7] A. Buffa and P. Monk, Error estimates for the ultra weak variational formulation of the Helmholtz equation. *ESAIM: M2AN* **42** (2008) 925–940.

[8] P. Castillo, B. Cockburn, I. Perugia and D. Schötzau, An a priori error analysis of the local discontinuous Galerkin method for elliptic problems. *SIAM J. Numer. Anal.* **38** (2000) 1676–1706.

[9] O. Cessenat, *Application d'une nouvelle formulation variationnelle aux équations d'ondes harmoniques.* Ph.D. Thesis, Université Parix IX Dauphine, Paris, France (1996).

[10] O. Cessenat and B. Després, Application of an ultra weak variational formulation of elliptic PDEs to the two-dimensional Helmholtz equation. *SIAM J. Numer. Anal.* **35** (1998) 255–299.

[11] O. Cessenat and B. Després, Using plane waves as base functions for solving time harmonic equations with the ultra weak variational formulation. *J. Comp. Acoust.* **11** (2003) 227–238.

[12] P. Cummings and X.-B. Feng, Sharp regularity coefficient estimates for complex-valued acoustic and elastic Helmholtz equations. *Math. Models Methods Appl. Sci.* **16** (2006) 139–160.

[13] B. Despres, Sur une formulation variationnelle de type ultra-faible. *C. R. Acad. Sci. Paris, Ser. I* **318** (1994) 939–944.

[14] C. Farhat, I. Harari and U. Hetmaniuk, A discontinuous Galerkin method with Lagrange multipliers for the solution of Helmholtz problems in the mid-frequency regime. *Comput. Methods Appl. Mech. Eng.* **192** (2003) 1389–1419.

[15] C. Farhat, R. Tezaur and P. Weidemann-Goiran, Higher-order extensions of a discontinuous Galerkin method for mid-frequency Helmholtz problems. *Int. J. Numer. Meth. Engr.* **61** (2004) 1938–1956.

[16] G. Gabard, Discontinuous Galerkin methods with plane waves for the displacement-based acoustic equation. *Int. J. Numer. Meth. Engr.* **66** (2006) 549–569.

[17] G. Gabard, Discontinuous Galerkin methods with plane waves for time-harmonic problems. *J. Comp. Phys.* **225** (2007) 1961–1984.

[18] C. Gittelson, R. Hiptmair and I. Perugia, *Plane wave discontinuous Galerkin methods.* Preprint NI07088-HOP, Isaac Newton Institute Cambride, Cambrid, UK (2007). Available at http://www.newton.cam.ac.uk/preprints/NI07088.pdf.

[19] U. Hetmaniuk, Stability estimates for a class of Helmholtz problems. *Communications in Mathematical Sciences* **5** (2007) 665–678.

[20] R. Hiptmair and P. Ledger, *A quadrilateral edge element scheme with minimum dispersion.* Report 2003-17, SAM, ETH Zürich, Zürich, Switzerland (2003).

[21] T. Huttunen and P. Monk, The use of plane waves to approximate wave propagation in anisotropic media. *J. Comput. Math.* **25** (2007) 350–367.

[22] T. Huttunen, P. Monk and J. Kaipio, Computational aspects of the ultra-weak variational formulation. *J. Comp. Phys.* **182** (2002) 27–46.

[23] T. Huttunen, M. Malinen and P. Monk, Solving Maxwell's equations using the ultra weak variational formulation. *J. Comp. Phys.* **223** (2007) 731–758.

[24] F. Ihlenburg, *Finite Element Analysis of Acoustic Scattering, Applied Mathematical Sciences* **132**. Springer-Verlag, New York (1998).

[25] O. Laghrouche, P. Bettes and R. Astley, Modelling of short wave diffraction problems using approximating systems of plane waves. *Int. J. Numer. Meth. Engr.* **54** (2002) 1501–1533.

[26] J. Melenk, *On Generalized Finite Element Methods.* Ph.D. Thesis, University of Maryland, USA (1995).

[27] P. Monk and D. Wang, A least squares method for the Helmholtz equation. *Comput. Methods Appl. Mech. Eng.* **175** (1999) 121–136.

[28] E. Perrey-Debain, O. Laghrouche and P. Bettess, Plane-wave basis finite elements and boundary elements for three-dimensional wave scattering. *Phil. Trans. R. Soc. London A* **362** (2004) 561–577.

[29] H. Riou, P. Ladevéze and B. Sourcis, The multiscale VTCR approach applied to acoustics problems. *J. Comp. Acoust.* (2008) (to appear).

[30] A. Schatz, An observation concerning Ritz-Galerkin methods with indefinite bilinear forms. *Math. Comp.* **28** (1974) 959–962.

[31] C. Schwab, *p- and hp-Finite Element Methods. Theory and Applications in Solid and Fluid Mechanics, Numerical Mathematics and Scientific Computation.* Clarendon Press, Oxford (1998).

[32] M. Stojek, Least-squares Trefftz-type elements for the Helmholtz equation. *Int. J. Numer. Meth. Engr.* **41** (1998) 831–849.

[33] R. Tezaur and C. Farhat, Three-dimensional discontinuous Galerkin elements with plane waves and lagrange multipliers for the solution of mid-frequency Helmholtz problems. *Int. J. Numer. Meth. Engr.* **66** (2006) 796–815.